

---

Masters Theses

Student Theses and Dissertations

---

Spring 2022

**COMPREHENSIVE EVALUATION OF NOVEL MEDIUM-  
TEMPERATURE AND HIGH-TEMPERATURE RESISTANT RE-  
CROSSLINKABLE PREFORMED PARTICLE GELS FOR  
CONFORMANCE CONTROL**

Zhanmiao Zhai

*Missouri University of Science and Technology*

Follow this and additional works at: [https://scholarsmine.mst.edu/masters\\_theses](https://scholarsmine.mst.edu/masters_theses)



Part of the [Petroleum Engineering Commons](#)

Department:

---

**Recommended Citation**

Zhai, Zhanmiao, "COMPREHENSIVE EVALUATION OF NOVEL MEDIUM-TEMPERATURE AND HIGH-TEMPERATURE RESISTANT RE-CROSSLINKABLE PREFORMED PARTICLE GELS FOR CONFORMANCE CONTROL" (2022). *Masters Theses*. 8141.

[https://scholarsmine.mst.edu/masters\\_theses/8141](https://scholarsmine.mst.edu/masters_theses/8141)

This thesis is brought to you by Scholars' Mine, a service of the Missouri S&T Library and Learning Resources. This work is protected by U. S. Copyright Law. Unauthorized use including reproduction for redistribution requires the permission of the copyright holder. For more information, please contact [scholarsmine@mst.edu](mailto:scholarsmine@mst.edu).

COMPREHENSIVE EVALUATION OF NOVEL MEDIUM-TEMPERATURE AND  
HIGH-TEMPERATURE RESISTANT RE-CROSSLINKABLE PREFORMED  
PARTICLE GELS FOR CONFORMANCE CONTROL

by

ZHANMIAO ZHAI

A THESIS

Presented to the Graduate Faculty of the  
MISSOURI UNIVERSITY OF SCIENCE AND TECHNOLOGY

In Partial Fulfillment of the Requirements for the Degree  
MASTER OF SCIENCE IN PETROLEUM ENGINEERING

2022

Approved by:

Baojun Bai, Advisor  
Ralph E. Flori Jr.  
Mingzhen Wei

© 2022

Zhanmiao Zhai

All Rights Reserved

## ABSTRACT

Gel treatment has been widely used to control excessive water production and improve oil recovery in mature oilfields. In comparison to traditional preformed particle gel (PPG), re-crosslinkable preformed particle gel (RPPG) has a significant advantage in treating abnormal features such as open fractures, fracture-like channels, and void space conduits (VSC). This research provides a comprehensive evaluation of two novel RPPG products developed in our lab: medium-temperature resistant RPPG (MT-RPPG) for a Middle East reservoir and a high-temperature resistant RPPG (HT-RPPG) for North Sea reservoirs (130 °C).

We assessed the effect of the monomer types and concentration, pH, salinity, and temperatures on swelling kinetics, as well as re-crosslinking time, gel strength, thermostability. The plugging efficiency was evaluated using the fractured cement model. For the MT-RPPG, results demonstrated that the elastic modulus of the MT-RPPG after re-crosslinking can reach up to 675 Pa at a swelling ratio of 1:10. The MT-RPPGs with the swelling ratios of 1:10, 1:20, and 1:30 have good thermostability in the injection water from the Middle East at 100 °C for over 150 days so far. The core flooding test showed that the breakthrough pressure was 118.2 psi/ft. For the environmentally friendly HT-RPPG, results showed that the HT-RPPG with a swelling ratio of 1:10 has the maximum G' of 460 Pa after re-crosslinking. The HT-RPPG with a swelling ratio of 1:10 has good long-term thermostability in North Sea formation water at 130 °C for over 208 days so far. Core flooding test showed that the breakthrough pressure was 68 psi/ft and the plugging efficiency is over 99.9%.

## ACKNOWLEDGMENTS

First and foremost, I want to express my gratitude to Dr. Baojun Bai, my advisor, for his persistent encouragement and assistance during my master's program. I have gained and improved my research abilities as a result of his patient instruction, time commitment, and motivation.

Second, I would like to thank my committee members, Dr. Ralph Flori and Dr. Mingzhen Wei, for their support, patience, valuable recommendations, and comments on my thesis.

I wish to express my thanks for the financial support from ConocoPhillips, Occidental Petroleum, and Daqing New Wantong Technology Developing Company.

I am sincerely grateful to Dr. Tao Song for his assistance and experiment design. He provided me with a great deal of support and guidance throughout the thesis. And special thanks to Dr. Shuda Zhao, Junchen Liu, Xuyang Tian, and Ya Yao for working with me and resolving my thesis difficulties.

Finally, I would like to express my gratitude to my loving family for their unwavering support and faith in me over the years.

## TABLE OF CONTENTS

	Page
ABSTRACT.....	iii
ACKNOWLEDGMENTS .....	iv
LIST OF ILLUSTRATIONS.....	viii
LIST OF TABLES .....	x
NOMENCLATURE .....	xi
 SECTION	
1. INTRODUCTION.....	1
2. LITERATURE REVIEW.....	3
2.1. ENHANCED OIL RECOVERY .....	3
2.2. RESERVOIR CONFORMANCE CONTROL PROBLEMS.....	5
2.2.1. Water Shutoff. ....	8
2.2.2. Profile Control.....	8
2.2.3. In-depth Fluid Diversion. ....	8
2.3. CONFORMANCE CONTROL USING GELS.....	9
2.3.1. In-situ Gel Technology.....	9
2.3.1.1. Metallic crosslinker.....	10
2.3.1.2. Organically crosslinker.....	11
2.3.2. Preformed Gel System.....	11
2.3.2.1. Preformed particle gels (PPGs).....	12

2.3.2.2. Bright water. ....	14
2.3.2.3. Nanocomposite preformed particle gel.....	15
2.3.2.4. Re-crosslinkable preformed particles gel (RPPG).....	16
3. EXPERIMENTAL MATERIALS AND PROCEDURES.....	18
3.1. MATERIALS.....	18
3.1.1. MT-RPPG.....	18
3.1.2. Environmentally Friendly HT-RPPG.....	19
3.2. RPPG SYNTHESIS.....	19
3.3. EVALUATION METHODOLOGIES.....	20
3.3.1. Swelling Capacity Measurement.....	20
3.3.2. Re-crosslinking Time Test. ....	20
3.3.3. Rheology Test and Linear Viscoelastic Region. ....	22
3.3.4. Thermostability Evaluation. ....	23
3.3.5. Plugging Efficiency valuation.....	23
4. SYNTHESIS AND EVALUATION OF MT-RPPG. ....	26
4.1. EFFECT OF MONOMERS ON RPPG PROPERTIES.....	26
4.2. EFFECT OF CROSSLINKER II ON RPPG PROPERTIES.....	26
4.3. EFFECT OF pH ON MT-RPPG.....	30
4.4. EFFECT OF CROSSLINKER I ON RPPG PROPERTIES.....	30
4.5. SWELLING KINETIC TEST.....	32
4.6. RHEOLOGY TEST.....	33
4.7. THERMOSTABILITY TEST.....	34

4.8. PLUGGING EFFICIENCY EVALUATION.....	36
5. SYNTHESIS AND EVALUATION OF ENVIRONMENTALLY FRIENDLY HT-RPPG .....	39
5.1. EFFECT OF CROSSLINKER II ON RPPG PROPERTIES.....	39
5.2. EFFECT OF PH ON RPPG PROPERTIES .....	42
5.3. EFFECT OF CROSSLINKER I ON RPPG PROPERTIES.....	44
5.4. SWELLING KINETIC TEST .....	46
5.5. RE-CROSSLINKING TIME TEST .....	47
5.6. RHEOLOGY TEST .....	48
5.7. THERMOSTABILITY TEST .....	49
5.8. PLUGGING EFFICIENCY EVALUATION.....	51
6. CONCLUSIONS .....	53
7. RECOMMENDATIONS .....	54
BIBLIOGRAPHY.....	55
VITA.....	61



**LIST OF ILLUSTRATIONS**

Figure	Page
2.1 Classification of oil recovery methods. ....	4
2.2 Classification of enhanced oil recovery methods. ....	4
2.3 Heterogeneity and high permeability channels problems during a waterflood. ....	7
2.4 Types of the conformance control techniques. ....	9
2.5 A process of a particle gel passing through a throat. ....	12
2.6 A process of particle gels through throats at the simplified model.....	13
3.1 Chemical structures of the compounds used in experiments. ....	18
3.2 The workflow of the synthesis and fabrication of the RPPG.....	19
3.3 The re-crosslinkable preformed particle gel re-crosslinking process. ....	21
3.4 Gel strength code. ....	21
3.5 HAAKE MARS III rheometer. ....	22
3.6 The laboratory core flooding test model.....	24
4.1 Dehydration of MT-RPPG with different AM/AMPS content.....	28
4.2 Dehydration of MT-RPPG with different concentrations of crosslinker II. ....	29
4.3 The effect of the concentration of MBA effect on the ESR of MT-RPPG.....	31
4.4 The effect of concentrations of MBA on the re-crosslinking time of MT-RPPG. ....	32
4.5 Effect of different types of salinities brine on swelling kinetics of the MT-RPPG.....	33
4.6 Effect of the swelling ratio on the elastic modulus of MT-RPPG. ....	34
4.7 Effect of aging time on the strength of MT-RPPG.....	35

4.8 The morphology of the MT-RPPG after aging test. ....	36
4.9 Water breakthrough pressure measurement for MT-RPPG during the core flooding test. ....	37
4.10 Residual resistance factor as a function of injection rate for MT-RPPG.....	38
5.1 The primary bulk gel with different weight ratios of monomers to crosslinker II. ....	40
5.2 Re-crosslinking behavior of the HT-4. ....	41
5.3 Effect of the weight ratios of monomers to crosslinker II on the elastic modulus of HT-RPPG.. ....	42
5.4 Effect of pH 4, 6, 7, and 8.....	43
5.5 The primary gel with different concentrations of MBA. ....	44
5.6 Effect of the concentration of MBA on the equilibrium swelling ratio of HT-RPPG.	45
5.7 Effect of the concentration of MBA on the gel strength of HT-RPPG.....	46
5.8 Effect of different types of salinities brine on swelling kinetics of the HT-RPPG.....	47
5.9 Effect of the temperature on the re-crosslinking time of the HT-RPPG with different swelling ratios .....	48
5.10 Effect of the temperature on the elastic modulus of the HT-RPPG with different swelling ratios. ....	49
5.11 The morphology of the HT-RPPG after aging test. ....	50
5.12 Retention volume of the HT-RPPGs with different swelling ratios at 80 °C, 100 °C, 120 °C, and 130 °C.....	50
5.13 Water breakthrough pressure measurement for HT-RPPG during the Core flooding test. ....	51
5.14 Residual resistance factor as a function of injection rate for HT-RPPG. ....	52

**LIST OF TABLES**

Table	Page
4.1 The effect of AM/AMPS content ratios on the strength of the primary gel and dehydration time (20%).....	27
4.2 The effect of the concentrations of crosslinker II on the strength of the primary gel and secondary gel. ....	29
4.3 The effect of the concentration of MBA on the strength of the primary gel and equilibrium swelling ratio. ....	30
5.1 Effect of the crosslinker II on the strength of the primary gel.....	40
5.2 Effect of the pH on the strength of the primary gel and re-crosslinking behavior of the HT-RPPG. ....	43
5.3 Effect of the concentration of MBA on the primary gel strength. ....	44

**NOMENCLATURE**

Symbol	Description
SR	Swelling ratio
ESR	Equilibrium swelling ratio
$V_s$	Volume of swollen gel
$W_i$	Weight of the dry RPPG particles
$G'$	Elastic modulus
$k_{\text{before}}$	Initial permeability of the fractured cement core
$d$	Width of the fracture
$k_{\text{after}}$	Permeability of the fractured cement core after the water breakthrough
$F_{rr}$	Residual resistance facto
$q$	Flow rate
$\mu$	Fluid viscosity
$L$	Length of the cement core
$A$	Cross-sectional area of the fracture
$\Delta P$	Variation of the pressure

## 1. INTRODUCTION

Excess water production is the major issue for most mature water flooding oilfields worldwide. Excess water production causes additional problems such as corrosion, scale, environmental concerns, and extra cost on the produced water treatment, and even eventually leading to well-shut in (Bai et al., 2013). According to the U.S report, the total amount of produced water associated with all onshore and offshore oil and gas production is approximately 21.2 billion barrels, with an average water-to-oil ratio of at least 10 barrels of water per barrel of oil in 2012 (Veil, 2015). Many techniques, such as polymer flooding, foam flooding, and gel treatment, have been developed to control excess water production and enhance oil recovery (Bai et al., 2004). Gel treatments have been extensively used as a cost-effective technique to control water production by injecting polymer gel into wells to fully or partially block high permeability zones (Zhao et al., 2006).

Two commonly gel systems that have been extensively utilized to control excessive water production are in-situ gels and preformed particles gels (PPGs). In-situ gel systems are composed of polymers and crosslinkers solutions. It can be injected into the formation sequentially or simultaneously to generate gels and entirely or partially block high-permeable water zones. The most extensively used in-situ gel system is the polyacrylamide (PAM)/Cr (III) system, which has a adjustable strength, good injectivity, and controllable gelation time (Sydansk, 1988). However, due to chromatographic separation, shear degradation, and adsorption, the polymer and crosslinker mixture (gelant) contents can alter, resulting in gelation failure. Furthermore, in-situ gels could

penetrate into low permeability oil-bearing zones, causing formation damage (Zhu et al., 2017).

Preformed particles gels (PPGs), pre-crosslinked at surface facilities, are another gel treatment system that can solve some limitations of in-situ gel system. The particles can swell a few to hundred times by absorbing the brine (Bai et al., 2004). The size and strength controllable PPGs can reduce the risk of formation damage in low permeability oil-bearing zones due to their large size compared to the rock pore size. However, several field experiments demonstrated that PPGs could not form efficient plugging for reservoirs with abnormal features, such as void space conduits (VSC) and large-opening fractures. Laboratory experiments also showed PPGs could be easily washed out from the fracture after the water breakthrough (Wang and Bai, 2018).

To solve the drawbacks of conventional PPGs, our group developed a novel re-crosslinkable preformed particle gel (RPPG) system, which can re-crosslink to produce a bulky gel. RPPG combines the benefits of in-situ gels and PPG, which have a relatively high mechanical strength and good transformability. However, the previous MT-RPPG has poor thermal stability in some formation water, and the previous HT-RPPG utilized an extremely expensive crosslinker with limited solubility in aqueous solutions.

This thesis provides a new MT-RPPG product with excellent salt resistance at medium temperature, which can be stable in a Middle East injection water. Besides, we also developed a new environmentally friendly HT-RPPG product for northsea reservoirs. The purpose of this thesis is to systematically assess the properties of the new RPPGs, such as swelling kinetics, rheological, re-crosslinking time, and thermal stability, and to observe if they can effectively plug the fractures at the target conditions.

## **2. LITERATURE REVIEW**

### **2.1. ENHANCED OIL RECOVERY**

Primary, secondary, and tertiary recoveries are the three main mechanisms in oil production process (Sheng, 2011). Figure 2.1 depicts the further classification of the three oil recovery mechanisms. For the primary recovery, the natural driving energy that already exists in the reservoir can push oil into the wellbore. The natural energies in primary recovery includes rock/fluid expansion, water influx, gravity drainage, gas cap, and solution gas (Sheng, 2011). Primary recovery can usually produce a small proportion of the original oil in place (OOIP), typically around 10-15%.

Secondary recovery is the recovery by the injection of the external fluid to maintain reservoir pressure and displace oil towards production wells. The most commonly applied secondary recovery techniques are water flooding and gas flooding. Primary and secondary recovery can usually account for about 35% of the OOIP due to the complicated conditions in a reservoir, such as reservoir heterogeneity, the presence of fractures or channels, high oil viscosity, and wettability (Green and Willhite, 1998).

Tertiary oil recovery, also known as enhanced oil recovery (EOR), involves extracting residual oil using materials which do not naturally occur in the reservoir (Green and Willhite, 1998). Common tertiary oil recovery techniques are chemical and thermal flooding, potentially producing 30-60% of the OOIP together with primary and secondary recovery.

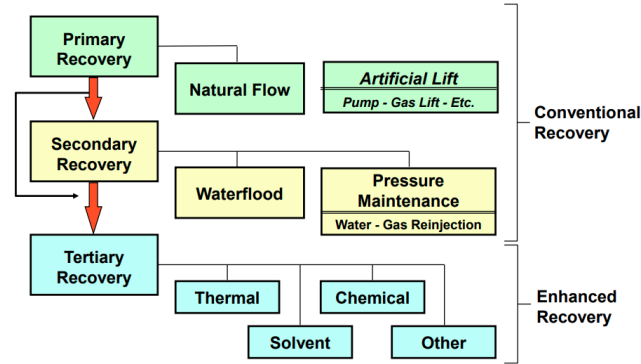


Figure 2.1 Classification of oil recovery methods(Oil & Gas Journal, 1990).

With rising energy demand, it is imperative to keep the sustained supplement of crude oil (Van Hung et al., 2020). Oil companies are interested in increasing oil recovery from mature reservoirs because mature fields account for most of the world's current oil production (Alvarado and Manrique, 2010). Therefore, enhanced oil recovery technologies are expected to become more important in energy balance. EOR aims to improve oil recovery by increasing microscopic displacement and volumetric sweep efficiency. Figure 2.2 summarizes the enhanced oil recovery methods.

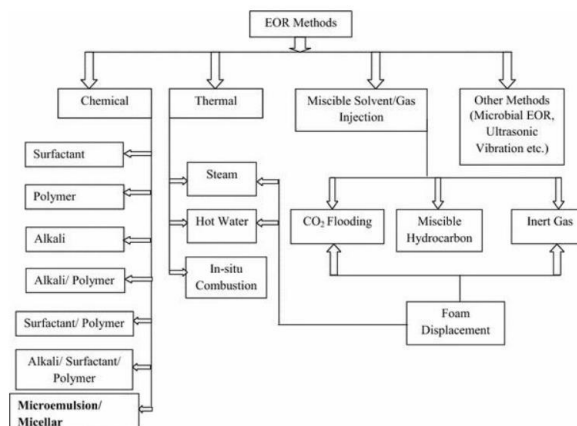


Figure 2.2 Classification of enhanced oil recovery methods (Bera and Mandal, 2015).



## 2.2. RESERVOIR CONFORMANCE CONTROL PROBLEMS

Conformance is a measuring volumetric sweep efficiency in any flooding oil production process (Sydansk and Romero-Zerón, 2011). Excessive water production is a common concern during the oil production process (Lantz and Muniz, 2014). Early water breakthrough and excessive water production have a detrimental effect on water/polymer flooding effectiveness. Figure 2.3 shows the problems of excessive water production due to the heterogeneity and high permeability channels during water flooding. Excessive water production leads to severe corrosion, scale, environmental issues (Bai et al., 2013). The average water-oil ratio in the United States is around eight (Al-Muntasheri, 2012). To control excessive water production and enhance sweep efficiency, it's critical to use the correct conformance improvement technique. From Bailey et al.'s (2000) summary, ten different conformance problems are associated with the near-wellbore and far-wellbore issues.

Casing, tubing, or packer leaks. A leak in the casing, tubing, or packer might cause water to flow directly to the wellbore and be produced (Bailey et al., 2000).

Channel flow behind the casing. The major cause of this issue is failing primary cementing, which connects the water-bearing zones to the pay zones (Bailey et al., 2000).

Moving oil-water contact. When the oil-water contact is close to the perforated zone and the vertical permeability of the formation is low, the oil-water contact may move up to the perforated zone, causing unwanted water to be produced (Bailey et al., 2000).

Watered-out layer without crossflow. There is a high permeability layer between two very low permeability shale layers, and there is no pressure connection between

them, resulting in this issue. The water will then tend to flow through the zone with high permeability (Bailey et al., 2000).

Fractures or faults between injector and producer. A naturally occurring fracture that connects the injection and production wells can result in a quick water breakthrough (Bailey et al., 2000).

Fractures or faults from a water layer. Natural fractures that penetrate the water-bearing zone might lead to water production (Bailey et al., 2000).

Coning or cusping. When the vertical permeability is high, oil-water contact occurs near the perforations. The oil-water contact can move upward as production rates increase. In vertical wells, it will lead to the coning problem, while in horizontal wells, it will lead to the cusping problem (Bailey et al., 2000).

Poor areal sweep. Reservoir heterogeneity can lead to the poor areal sweep problem during waterflooding through a pay zone (Bailey et al., 2000).

Gravity-segregated layer. This issue manifests itself in the thick high permeability layer. Water only sweeping the lower half of the formation can result in unwanted water production (Bailey et al., 2000).

Watered-out layer with crossflow. This problem is similar to the watered-out layer without crossflow problem. The distinction is there is crossflow between the layers which can lead to pressure communication between them (Bailey et al., 2000).

Conformance control techniques can be categorized as mechanical, completion, and chemical methods (Sydansk and Romero-Zerón, 2011).

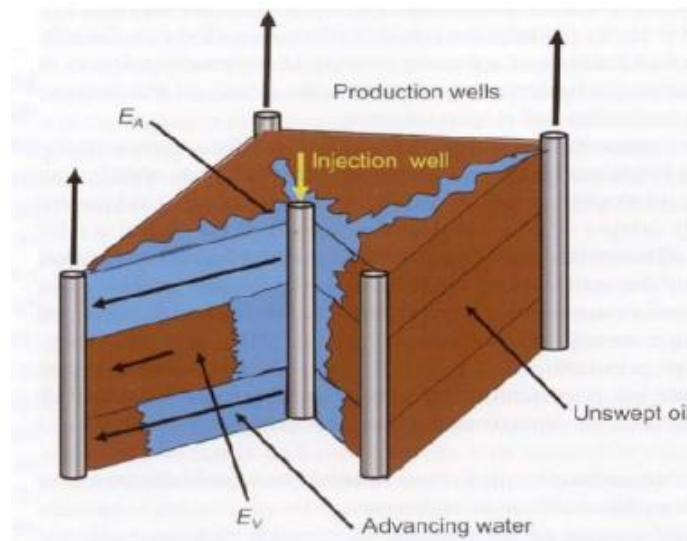


Figure 2.3 Heterogeneity and high permeability channels problems during a waterflood (Sydansk and Romero-Zerón, 2011).

Mechanical methods usually use hardware such as packers, cement, plugs, and patches to solve the near-wellbore issues like channel flow behind casing, casing/tubing/packer leaks, watered-out layer without crossflow, and moving oil-water contact. Completion methods use sidetracks, multilateral wells, dual completions, and coiled-tubing may effectively solve problems like poor areal sweep, gravity-segregated layer, and conning or cusping (Bailey et al., 2000).

Mechanical and completion methods can be employed to treat some types of near-wellbore problems, but they have limitations and cannot address all the excessive water production issues.

Chemical methods can be divided into water shutoff, profile control, and in-depth fluid diversion treatment. Figure 2.4 shows the three different types of conformance control techniques (Liu et al., 2006).

**2.2.1. Water Shutoff.** This technique utilizes a plugging agent to plug or selectively block water production from high permeability zones in the production well (Liu et al., 2006). It can be classified as non-selective or selective treatments depending on the reservoir situation. When there is an impermeable layer between the low and high permeability layers, non-selective treatment can be used to divert the injected water towards the oil zones with low permeability. Sealing materials may damage the oil-bearing zones if there is vertical connectivity between the oil and water zones. Selective water shutoff treatments can be employed as relative permeability modifiers to lower water permeability more than oil (Liu et al., 2010). The water shutoff is applied in the reservoir's early stages.

**2.2.2. Profile Control.** This technology injects polymer gels such as acrylamide-based gels, silicate gels, etc., into the injection wells to plug high permeability water areas. The profile control technique is applied in the middle stages of reservoir production. In addition, profile control can be combined with the water shutoff simultaneously (Liu et al., 2006).

**2.2.3. In-depth Fluid Diversion.** For water shutoff and profile control techniques, gels are typically placed near the wellbores to improve reservoir conformance. The in-depth fluid diversion technique involves the injection of a large volume of plugging agents into the reservoir, forming in-depth plugging and physically diverting the post-injected fluid to unwept oil-rich zones (Liu et al., 2006; Bai et al., 2008). Some polymer gels, such as CDG and weak gel, have been widely used for in-depth fluid diversion (Bai et al., 2015).

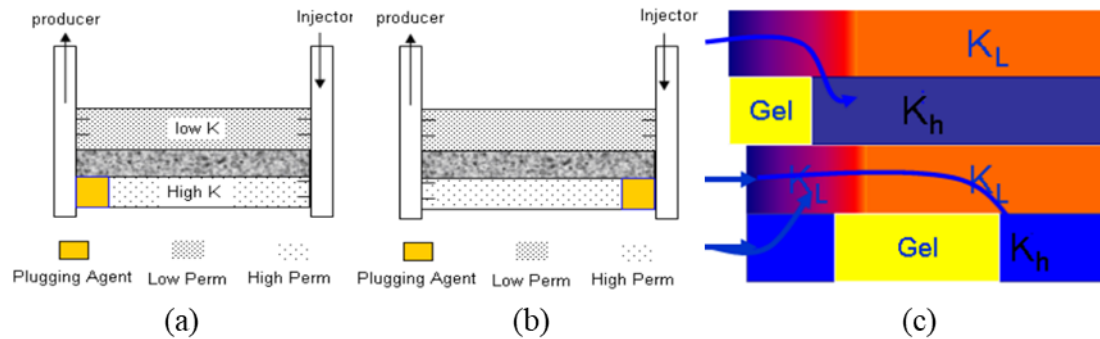


Figure 2.4 Types of the conformance control techniques (Liu et al., 2006).  
 (a) Water shutoff, (b) profile control, (c) in-depth fluid diversion.

### 2.3. CONFORMANCE CONTROL USING GELS

Gel treatment is an effective and low-cost technique for sealing the thief zone and diverting water into the oil-bearing area. It has been extensively employed to control water production (Bai et al., 2015). Gel types can be categorized by in-situ gel technology and preformed gel technology (Bai et al., 2015).

**2.3.1. In-situ Gel Technology.** The in-situ gel system is the most extensively used gel technology in the oilfields to treat conformance control issues. Gelant, a mixture of polymer and crosslinker solutions, is injected into the formation to create an in-situ three-dimensional network that seals the target formation under reservoir conditions (Moradi-Araghi, 2000).

Several types of polymers and crosslinkers have been developed. In the oil industry, synthetic polymers such as polyacrylamide and biopolymers such as starch, xanthan gum, guar, and cellulose were commonly used (Bai et al., 2015). Partially hydrolyzed polyacrylamide (HPAM) is the most widely utilized polymer in all gel

systems. Crosslinkers are classified into two types: metallic crosslinked systems and organically crosslinked systems (Ghriga et al., 2019).

**2.3.1.1. Metallic crosslinker.** The multivalent metal cations (aluminum, chromium, ferric, boron, and zirconium) can form ionic bonding with the negatively charged groups of the polymers to generate gels. The crosslinking rate between the metallic cations and polymer chains is controlled by the ligands exchanging rate (Sydansk, 1990; Bai et al., 2015). The crosslinking rate can be delayed by adding extra ligands such as acetate and lactate.

Aluminum sulfate was employed to crosslink HPAM in the early 1970s (Scoggins and Miller, 1979). However, this substance is highly pH-dependent, and the gelant might lose crosslinking ability after contacting formation water. As a result, HPAM/aluminum sulfate can only be used to treat the area near the wellbore (Bai et al., 2015).

The HPAM/Cr (VI) gel system used extensively in oilfields owing to the controllable crosslinking time about twenty year ago (Nanda et al., 1987). However, Cr (IV) is a carcinogen, and the gel is sensitive to reservoir interference (Bai et al., 2015). Sydansk patented a gel system that used Cr (III) and HPAM to form the aqueous gels for conformance control (Sydansk, 1988). Additionally, The HPAM/Cr (III) gel system is insensitive to pH and salinity. In addition, it can also be applied in high-temperature reservoirs by using concentrated low molecular weight polymer and concentrated crosslinker (Sydansk, 1993). Many oilfields have achieved significant success with this gel system (Bai et al., 2015).

**2.3.1.2. Organically crosslinker.** Several organic crosslinkers can also crosslink the acrylamide-based polymers, and the crosslinked gel tends to have much better thermal stability than the gels crosslinked by the metallic crosslinkers. Chang et al. utilized formaldehyde and phenolic compounds to crosslink polyacrylamide (Chang et al., 1985). According to Seright et al., the gelation time of formaldehyde-based crosslinker is susceptible to salinity and pH, and the gelation does not occur at pH below 7.5. Morgan et al. developed a new organically polyethyleneimine (PEI)/PAM system that can be employed in high-temperature reservoirs (Morgan et al., 1997). This PEI-based gel system has been successfully used for water shutoff (Hardy et al., 1999).

Limitation of in-situ gel system. In some cases, gelant may flow into the low permeability oil-bearing zones and cause formation damage (Liang et al., 1993). Another limitation of the in-situ gel system is the dilution of gelant by the formation water, and the gelant might lose gelation ability after the dilution (Young et al., 1988).

**2.3.2. Preformed Gel System.** Another gel technology is the preformed gel system, which forms the gel at the surface facilities. The preformed gel system is less likely to cause formation damage due to the large particle compared to the rock pore size. Several types of preformed gels, such as preformed particle gel (PPG), microgels, submicron-sized particle gels (Bright Water), nanocomposite preformed particle gels, and re-crosslinkable preformed particle gels (RPPG), have been developed (Coste et al., 2000; Bai et al., 2007a; Chauveteau et al., 1999; Pritchett et al., 2003; Frampton et al., 2004; Pu et al., 2019).

**2.3.2.1. Preformed particle gels (PPGs).** Bai et al. (2004) developed the preformed particle gels, which are millimeter-sized gel particles resistant to salinity and temperature. It has been applied in China to address the excessive water production issues of mature reservoirs (Coste et al., 2000; Bai et al., 2007b). The gel particles can absorb brine and swell (Bai et al., 2007b). The swelled particles, which are deformable and elastic, can then migrate into the formation and fully or partially plug the high permeability channels (Coste et al., 2000; Bai et al., 2007b). Based on experimental observations, Bai et al. identified six types of PPG transporting mechanisms in porous media: direct pass, adsorption, trap, shrink and pass, deform and pass, and snap-off (Bai et al., 2007b). Figure 2.5 and Figure 2.6 show the process of particle gels passing through the pore throat at different models.

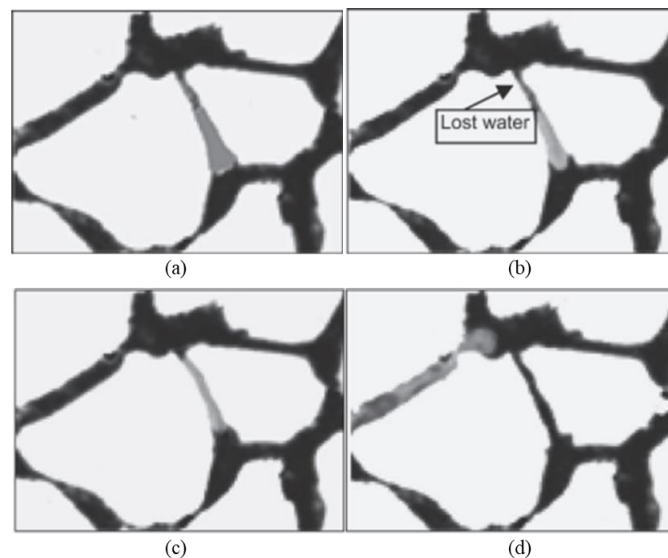


Figure 2.5 A process of a particle gel passing through a throat. (a) PPG moving to throat entrance, (b) squeezed water from PPG, (c) stretched particle filling throat, (d) particle passing through the throat (Bai et al., 2007b).



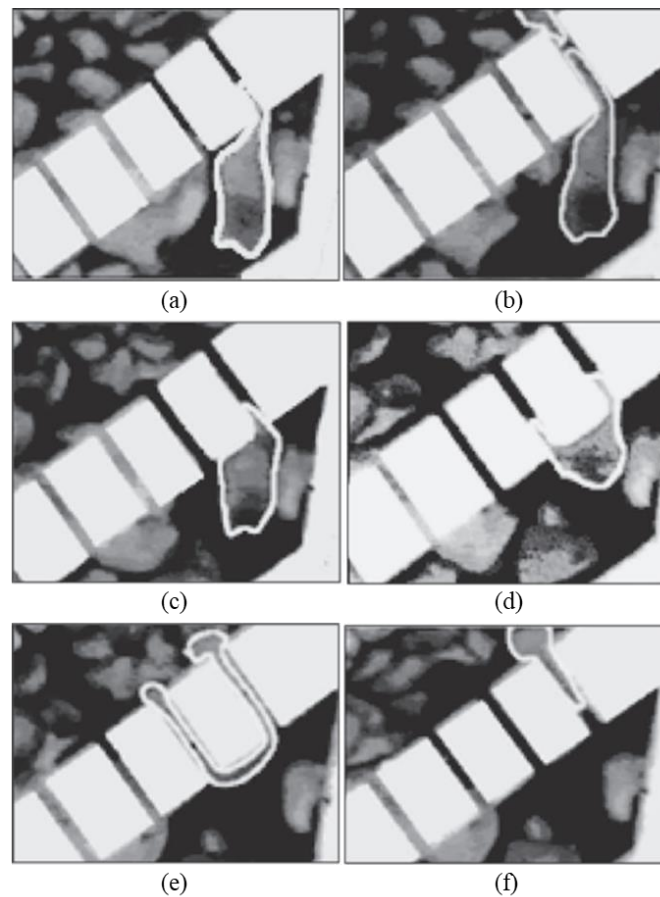


Figure 2.6 A process of particle gels through throats at the simplified model. (a) PPG moved to the throat, (b) PPG was broken into two particles, (c) the larger part tried to pass through the throat, (d) PPG became more arched, (e) Two ends of PPG particle enter two throats, (f) PPG was broken again and passed through the throat (Bai et al., 2007b).

Qiu et al. reported that PPGs had been successfully implemented in mature oilfields and fractured reservoirs in China to increase oil recovery (Qiu et al., 2014). On the other hand, PPGs are restricted to apply in reservoirs with fractures-like channels or fractures due to their bigger particle size and relatively fast swelling kinetics.

**2.3.2.2. Bright water.** BP, Chevron, Texaco, and Nalco collaborated to develop a submicron-sized particle gel system known as BrightWater (Frampton et al., 2004; Pritchett et al., 2003). The BrightWater system was a small, highly swellable particle gel that could move deep into the formation to plug high permeability thief zones and enhance oil displacement efficiency (Frampton et al., 2004; Pritchett et al., 2003). The BrightWater system consists of sulfonated polyacrylamide crosslinked with both labile and stable crosslinkers. The inverse emulsion polymerization method is used to synthesize the BrightWater, which ensures a narrow particle size distribution. When the gels are injected into the formation, the labile crosslinker begins to break as the temperature rises. That leads the gel to swell by absorbing the surrounding fluid while the stable crosslinker keeps the gels network intact. Therefore, BrightWater is also known as thermally activated polymers (Bai et al., 2015).

According to Pritchett et al., (2003), the first field application of BrightWater was in Minas, Indonesia. They demonstrated no injection issue when a low viscosity slug of BrightWater was injected into the reservoir. Furthermore, they confirmed the BrightWater could improve the injection profile and propagate deep into the formation (Pritchett et al., 2003). The first commercial implementation of BrightWater was successful in Alaska, with 60,000 bbls of oil recovered incrementally (Ohms et al., 2010). However, BrightWater is a mixture of particles and surfactants, and it is difficult to determine which component is responsible for the improved oil recovery. Furthermore, due to its narrow application range and poor thermal stability, this gel system is only employed in restricted conditions (Bai et al., 2015).

**2.3.2.3. Nanocomposite preformed particle gel.** Conventional polymer gels are unstable in severe reservoir conditions such as high salinity and temperature (Cordova et al., 2008; Johnson et al., 2010; Singh et al., 2018). Several methods have been used to enhance the thermal and phase stability of the polymer gels. Over the last few years, nanocomposites have attracted the oil field industry (Peng et al., 2018). Several authors investigated the use of nanomaterials to improve the thermal stability and strength of preformed particle gels to satisfy the requirements of water plugging in hostile environments. Montmorillonite, laponite clays, kaolinite clays, fly ash, starch, silicon dioxide, and aluminum dioxide are all commonly utilized nanomaterials to improve the properties of preformed particle gels (Darvishi et al., 2011; Tongwa and Bai, 2014; Kumar et al., 2019; Long et al., 2019; Saghafi et al., 2016). According to Salimi et al. (2014), applying montmorillonite clay to a gel system can improve the gel elastic properties and delay the onset of thermal degradation (Salimi et al., 2014). Singh et al. (2018) discovered that adding fly ash to gels system can increase their strength and extend their gelation time, resulting in better plugging efficiency (Singh et al., 2018).

Clay dispersion is important to the success of any nanocomposite gel formation. The mixing process of the polymer and clay can be described in three ways: unmixed, intercalated, and exfoliated. Clay layers are pulled apart during the intercalated process, and polymer chains are not jointed with clay layers. Until the exfoliated stage, when the individual clay layers are separated wide apart and jointed with polymer chains to improve the strength of the gel system (Tongwa et al., 2013). PPGs produced by sodium montmorillonite can resist temperatures of up to 145 °C, according to Saghafi et al. (2016). However, the long-term stability of the nanocomposite preformed particle needs

to be investigated (Long et al., 2019; Saghafi et al., 2016). It is also necessary to evaluate the effect of nanomaterials on other properties of the preformed particle, such as relative permeability reduction and propagation through porous media.

**2.3.2.4. Re-crosslinkable preformed particles gel (RPPG).** In mature oilfields, preformed particle gels have been employed to treat conformance control problems. However, according to Pu et al. (2019), oilfield trials have shown that preformed particle gels cannot effectively plug fracture-like channels, open fractures, and void space conduits (VSC) in many mature oilfields (Pu et al., 2019). Oilfield trials have demonstrated that PPGs are ineffective for plugging reservoirs with an 85% or higher water cut (Qiu et al., 2017). Furthermore, the mechanical properties of PPGs are easily changed by reservoir temperatures, brine salinity, and formation matrix composition (Bai et al., 2007a). Laboratory experiments indicated that PPGs could easily be washed out from the fractures after the breakthrough (Wang and Bai, 2018). As a result, the new re-crosslinkable preformed particles gel (RPPG) system was developed to address the conformance control issues associated with the abnormal features in mature oilfields (Pu et al., 2019).

The distinction between RPPG and PPG is that RPPG can re-crosslink to form a bulk gel after being injected into the formation (Pu et al., 2019). The purpose of developing RPPGs was to extend the longevity of the fracture or void space conduit plugging treatment (Targac et al., 2020). Dual-crosslinking chemistries were used to develop re-crosslinkable preformed particle gels. Crosslinker I is employed to crosslink the polymer chains and generate insoluble gel particles, whereas crosslinker II endows the gel system with re-crosslinking capabilities. After being placed in the fractures, the

swelled gel particles can re-crosslink to form a bulky gel. The gelation time of the RPPGs during their transport through the formation can be controlled, and all the components in the package will migrate together, avoiding chromatographically separated issues (Pu et al., 2019). Compared to conventional PPGs, lab test shows that RPPGs are more effective in plugging open fractures (Pu et al., 2019). The LT-RPPG can be used in reservoirs with temperatures ranging from 20 to 80 °C. Yu et al. developed novel high-temperature resistant RPPGs with better thermal stability under high temperatures. The crosslinked polymer gel was stable for over 200 days at 130 °C in North Sea formation water with a swelling ratio of 10 (Yu et al., 2022).

Current MT-RPPG has poor thermal stability in Middle East injection water. Severe syneresis or dehydration can be observed after ten days of aging at 100 °C. This thesis aims to develop and evaluate a novel MT-RPPG product that can be stable in Middle East injection water and has good fracture plugging efficiency. In addition, the previous HT-RPPG utilized an extremely expensive secondary crosslinker with limited water solubility, which increased the difficulties during pilot production. Therefore, this work aims to develop a cost-effective and easy fabricating HT-RPPG for conformance control in the North Sea high-temperature reservoirs (130 °C).

### 3. EXPERIMENTAL MATERIALS AND PROCEDURES

#### 3.1. MATERIALS

This section introduces the chemical materials used to synthesize MT-RPPG and Enviromentally Friendly HT-RPPG products.

**3.1.1. MT-RPPG.** Acrylamide (AM), 2-acrylamido-2-methylpropane sulfonate (AMPS), Ammonium persulfate (APS), N, N'-methylenebisacrylamide (MBA), Chromium (III) chloride hexahydrate ( $\text{CrCl}_3 \cdot 6\text{H}_2\text{O}$ ) and other inorganic salts were purchased from Sigma-Aldrich (St. Louis, MO) and the structures are showed in Figure 3.1. Distilled water was used for the polymer synthesis.

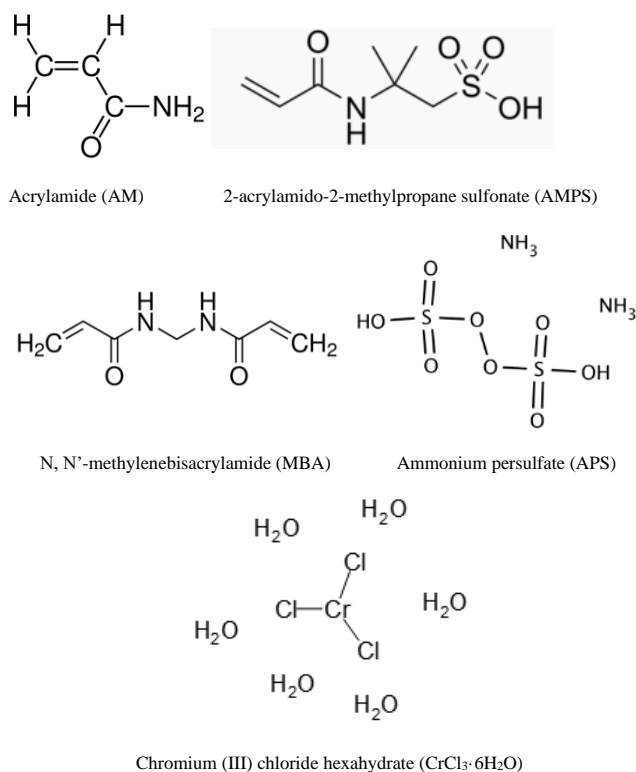


Figure 3.1 Chemical structures of the compounds used in experiments.

**3.1.2. Environmentally Friendly HT-RPPG.** Crosslinker II was purchased from Sigma-Aldrich (St. Louis, MO).

### 3.2. RPPG SYNTHESIS

Re-crosslinkable preformed particle gels were synthesized through aqueous free-radical polymerization. Figure 3.2 below shows the workflow of the synthesis and fabrication of the RPPG. The following example illustrates the synthesis process for re-crosslinkable preformed particle gels. Monomers were dissolved in distilled water in a beaker at first. Then, the preweight crosslinkers were added to the solution and mixed. The initiator was introduced after the solution was purged with argon for 5 minutes. The solution was then purged with argon for another 5 minutes. After that, the solution was heated in a pre-heated oven at the desired temperature for 8 hours to get a bulk gel. The bulk gel was then cut into small pieces and air-dried. Finally, the dried gel solids were crushed and sieved to the desired particle sizes.

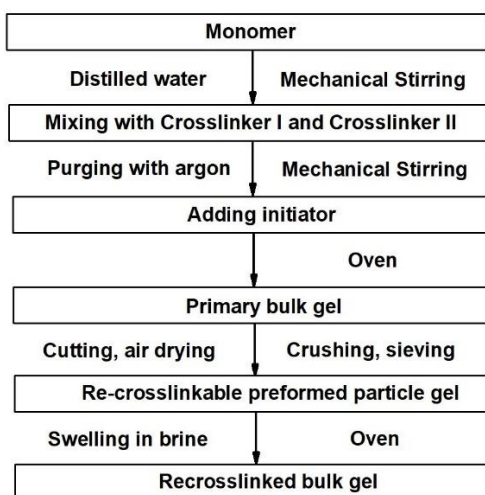


Figure 3.2 The workflow of the synthesis and fabrication of the RPPG.

### 3.3. EVALUATION METHODOLOGIES

This section introduces the evaluation methodologies used to evaluate the properties of RPPGs.

**3.3.1. Swelling Capacity Measurement.** The swelling kinetics were studied by immersing the dried gel particles into different brines and recording the gel volume changes as a function of time. In addition, the equilibrium swelling ratio (ESR) was also recorded. The weight of the RPPG particles before swelling was defined as  $W_i$ . The volume of the swelled gel particles was defined as  $V_s$ , and the swelling ratio (SR) was calculated using the Equation. (1).

$$SR = \frac{V_s}{W_i} \quad (1)$$

**3.3.2. Re-crosslinking Time Test.** The re-crosslinking time of the RPPGs was investigated using the bottle-test method (Sydansk, 1988). First, the dry RPPGs particles were swelled in the deoxygenated brine and sealed in high temperature-resistant glass tubes. After absorbing all the brine, the glass tubes were placed in the pre-heated ovens. For the MT-RPPG and HT-RPPG, the testing temperatures were 100 and 130 °C, respectively. We also tested the crosslinking behavior of HT-RPPG at 80 and 100 °C. The morphology of the gels was checked periodically to assess the re-crosslinking behavior. The re-crosslinking start time was defined as when the particle boundary began to disappear. The crosslinking ending time was defined as when all particle boundaries disappeared. Figure 3.3 shows the RPPG re-crosslinking process. The gel strength was evaluated using the gel strength code, as shown in Figure 3.4 (Sydansk, 1988).



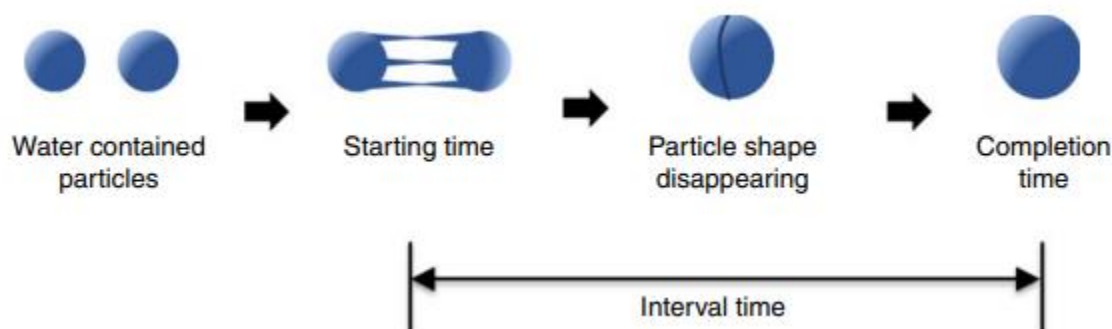


Figure 3.3 The re-crosslinkable preformed particle gel re-crosslinking process.

TABLE 1—BOTTLE-TEST GEL STRENGTH CODES	
A	<i>No detectable gel formed.</i> The gel appears to have the same viscosity (fluidity) as the original polymer solution and no gel is visually detectable.
B	<i>Highly flowing gel.</i> The gel appears to be only slightly more viscous than the initial polymer solution.
C	<i>Flowing gel.</i> Most of the obviously detectable gel flows to the bottle cap upon inversion.
D	<i>Moderately flowing gel.</i> A small portion (about 5 to 15%) of the gel does not readily flow to the bottle cap upon inversion—usually characterized as a “tonguing” gel (i.e., after hanging out of the bottle, gel can be made to flow back into the bottle by slowly turning the bottle upright).
E	<i>Barely flowing gel.</i> The gel slowly flows to the bottle cap and/or a significant portion (> 15%) of the gel does not flow upon inversion.
F	<i>Highly deformable nonflowing gel.</i> The gel does not flow to the bottle cap upon inversion (gel flows to just short of reaching the bottle cap).
G	<i>Moderately deformable nonflowing gel.</i> The gel flows about halfway down the bottle upon inversion.
H	<i>Slightly deformable nonflowing gel.</i> Only the gel surface deforms slightly upon inversion.
I	<i>Rigid gel.</i> There is no gel-surface deformation upon inversion.
J	<i>Ringing rigid gel.</i> A tuning-fork-like mechanical vibration can be felt after the bottle is tapped.

Figure 3.4 Gel strength code (Sydansk, 1988).

### 3.3.3. Rheology Test and Linear Viscoelastic Region. HAAKE MARS III

rheometer (Thermo Scientific Inc.) and the spindle is PP35L Ti L with the gap of 1 mm were used to measure the elastic modulus ( $G'$ ) of the re-crosslinked RPPG (Figure 3.5). The re-crosslinked RPPGs samples were cut into pieces of about 2 cm in diameter and 1.5 mm in height and then placed in the rheometer at room temperature (23 °C). The strain sweep test was used to perform the elastic modulus ( $G'$ ) of the RPPG as a function of strain with a fixed frequency of 1 Hz to measure the linear viscoelastic region of the re-crosslinked RPPG to show that the strain of 1% was in the linear viscoelastic region. Then, the elastic modulus ( $G'$ ) and viscous modulus ( $G''$ ) were obtained as a function of time, using an oscillation time-dependent experiment model with a fixed frequency of 1 Hz and a controlled strain of 1%.

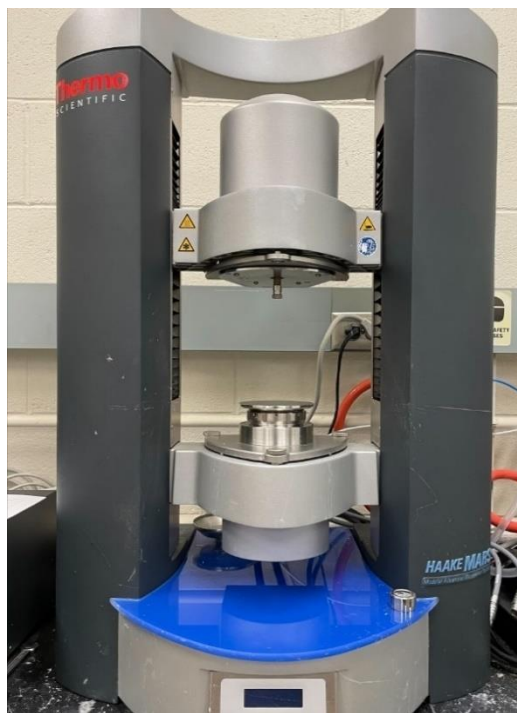


Figure 3.5 HAAKE MARS III rheometer.

**3.3.4. Thermostability Evaluation.** The volume and morphological of the re-crosslinked RPPGs were monitored under various brines and temperatures. Argon was pumped into the tubes for 20 minutes to remove the oxygen. The high-pressure glass tube was placed on the shaker until no free water was visible, then the glass tubes were placed in the pre-heated oven. For the MT-RPPG, several brines such as 1% NaCl, Middle East injection water, 5% CaCl<sub>2</sub>, and 10% CaCl<sub>2</sub>, were employed for the stability tests, and the swelling ratio ranges from 10 to 30. For the Environmentally Friendly HT-RPPG, the gels were swelled in 1% NaCl, 2% KCl, and North Sea formation water, and the swelling ratios were 10, 20, and 30.

**3.3.5. Plugging Efficiency Evaluation.** The laboratory core flooding test was used to assess the plugging efficiency of RPPG. Portland cement was utilized to prepare a fractured core. To create the fracture, the prepared cement slurry was poured into a cylindrical mold with a diameter of 5.08 cm, and a stainless-steel strip with a thickness of 0.30 cm was placed vertically in the center of the mold. The core is 8.89 cm in length, and the fracture width is 0.30 cm. The apparatus of the cement core is shown in Figure 3.6. The initial permeability of the fractured cement core was calculated by using the Equation. (2).

$$k_{\text{before}} = \frac{d^2}{12} \quad (2)$$

where  $k_{\text{before}}$  is the initial permeability of the fractured cement core, and  $d$  is the width of the fracture.

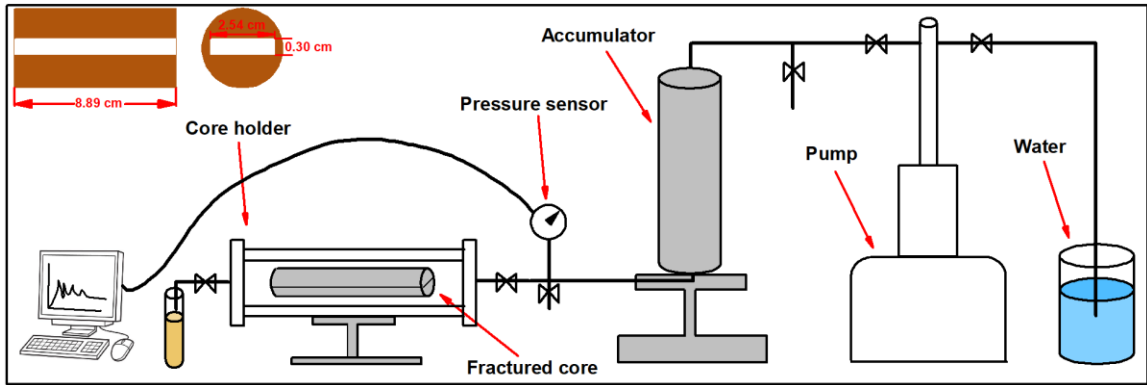


Figure 3.6 The laboratory core flooding test model.

The RPPG particles were swelled in 1% NaCl brines with a swelling ratio of 1:10. After the RPPG absorbed all of the brine, the RPPG dispersion was injected into the fracture at a constant flow rate of 1.0 mL/min until the pressure was stable. After that, a high-pressure resistant stainless-steel vessel was used to seal the cement core, and the vessel was aged at the appropriate temperature to cure the RPPG fully. The aging temperature of MT-RPPG and HT-RPPG were 100 and 130 °C, respectively.

The breakthrough test was evaluated using a constant flow rate method. The flow rate was set at 0.5 mL/min. After the water breakthrough, the pump was changed to constant injection mode with an injection rate of 0.1 ml/min until the pressure was stable. The injection flow rate was then changed to 0.25, 0.5, and 1.0 ml/min, and the stable pressure under each flow rate was recorded to calculate the residual resistance factor ( $F_{rr}$ ).  $F_{rr}$ , was calculated using the Equation. (3). below.

$$F_{rr} = \frac{k_{\text{before}}}{k_{\text{after}}} \quad (3)$$

where  $k_{\text{before}}$  is the initial permeability of the fractured cement core and  $k_{\text{after}}$  is the permeability of the fractured cement core after the water breakthrough that can be calculated by Darcy's law equation (Darcy, 1856).

$$k = \frac{q\mu L}{A\Delta P} \quad (4)$$

where  $q$  is the flow rate ( $\text{cm}^3/\text{s}$ ),  $\mu$  is the fluid viscosity (cp),  $L$  is the length (cm) of the cement core,  $A$  is the cross-sectional area ( $\text{cm}^2$ ) of the fracture and  $\Delta P$  is the variation of the pressure (atm).

To better describe the plugging efficiency of the RPPGs, the plugging efficiency can be calculated by the Equation. (5). (SONG et al., 2010).

$$\text{Plugging Efficiency} = \left(1 - \frac{1}{F_{rr}}\right) \times 100\% \quad (5)$$

## **4. SYNTHESIS AND EVALUATION OF MT-RPPG**

### **4.1. EFFECT OF MONOMERS ON RPPG PROPERTIES**

Under high temperatures, homo-polyacrylamide is extremely unstable at temperatures higher than 80 °C. Besides, PAM suffers extensive hydrolysis, and precipitations can be observed in the presence of divalent cations such as  $\text{Ca}^{2+}/\text{Mg}^{2+}$  (Stahl and Schulz, 1988). In this work, the anionic monomer-AMPS was utilized as a comonomer, which has better thermal stability and salt resistance than AM (Moradi-Araghi et al., 1987; Jouenne, 2020).

### **4.2. EFFECT OF CROSSLINKER II ON RPPG PROPERTIES**

Chromium (III) chloride hexahydrate ( $\text{CrCl}_3 \cdot 6\text{H}_2\text{O}$ ) was chosen as the secondary crosslinker to endow the MT-RPPG with the re-crosslinking ability. Several  $\text{Cr}^{3+}$  based polymers gels were synthesized to test the thermostability and strength of the primary gels in order to investigate the influence of  $\text{CrCl}_3 \cdot 6\text{H}_2\text{O}$  and AM/AMPS molar ratio on the properties of the MT-RPPGs. The total monomer weight was fixed to 30 grams, and 100 g of distilled water was used to dissolve all the monomers and crosslinkers. First, the weight ratio of monomers to  $\text{Cr}^{3+}$  was set to 200:1. Then, we set various AM/AMPS molar ratios to 10:0, 9:1, 8:2, 6:4, 4:6, and 2:8. The strength of the primary gels was recorded after polymerization. The thermal stability was carried out in Middle East injection water and lasted for over 100 days.

Table 4.1 shows the strength of the primary gel and the dehydration time (20% volume change of the gel) of the MT-RPPG with the swelling ratio of 1:30 in Middle East injection water at 100 °C.

Table 4.1 The effect of AM/AMPS content ratios on the strength of the primary gel and dehydration time (20%).

#	AM: AMPS	1 <sup>st</sup> gel	Dehydration time (20%) /SR-30 in Middle East injection water
MT-1	10:0	Very strong	24
MT-2	9:1	Very strong	38
MT-3	8:2	Strong	50
MT-4	6:4	Medium strong	No dehydration after 140 days and remained Code I
MT-5	4:6	Sticky	No dehydration but change to Code A after 68 days
MT-6	2:8	Flowing	No dehydration but change to Code A after 24 days

The gel strength of the 1<sup>st</sup> gel gradually decreases with the increase of AMPS concentration. The 1<sup>st</sup> gel became amorphous when the AMPS concentration was higher than 40%. However, the thermal stability of the re-crosslinked gel increased with AMPS concentration. Figure 4.1 shows the dehydration of the gels with different AMPS concentrations. Severe syneresis was observed for the gels with 0, 10, and 20% of AMPS after two months of aging, and the re-crosslinked gel lost over 30% of its original volume. It should also be mentioned that the elastic modulus of the re-crosslinked decreased with the increase of the AMPS concentration. The re-crosslinked gel with 40%

of AMPS remained stable for over 140 days in Middle East injection water. However, the re-crosslinked gel changed to a highly flowing gel when the AMPS concentration was 60 and 80%. The average molecular weight decreases with the increase of AMPS. In addition, the AMPS is insensitive to the pre-embedded crosslinker. Therefore, the re-crosslinking density is not dense enough to maintain the long-term mechanical integrity of the re-crosslinked gel. Furthermore, the chain repulsion also increases with AMPS concentration, hindering the chain-chain entanglement and re-crosslinking. Therefore, the optimized monomer recipe is 60% AM and 40% AMPS.

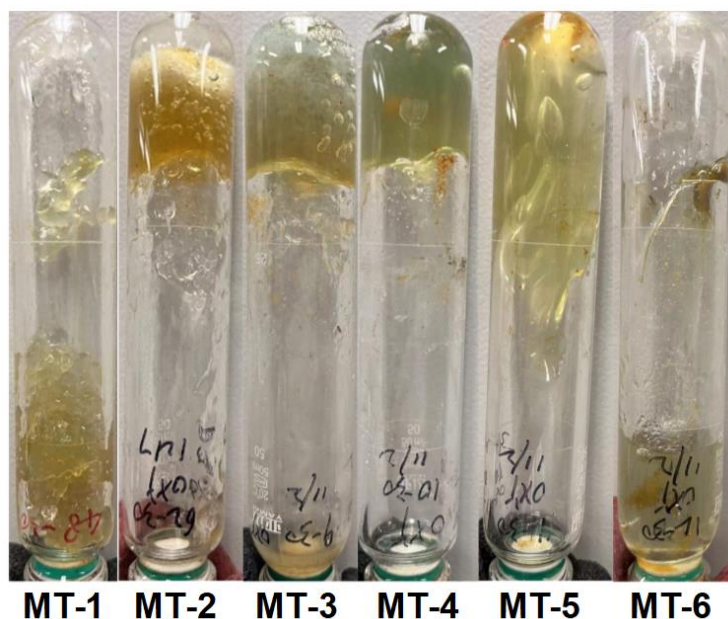


Figure 4.1 Dehydration of MT-RPPG with different AM/AMPS content.

Table 4.2 shows the effect of crosslinker II concentration on the thermal stability and strength of the re-crosslinked gel. The re-crosslinked gel strength gradually increases with the Cr (III) concentration. The re-crosslinked gel cannot reach gel code I when the



monomer to Cr (III) weight ratio is higher than 200:1. However, severe syneresis can be observed when the Cr (III) concentration is too high as shown in Figure 4.2. For example, MT-10 with a monomer to Cr (III) weight ratio of 50:1 began to syneresis after 15 days of aging. Therefore, the optimized monomer to Cr (III) weight ratio was 200:1.

Table 4.2 The effect of the concentrations of crosslinker II on the strength of the primary gel and secondary gel.

#	M: Cr <sup>3+</sup>	1 st gel	Note secondary gel, thermal stability same as above
MT-7	600:1	Medium strong	Low mechanical strength, lack of crosslinking
MT-8	300:1	Medium strong	Medium mechanical strength, good thermal stability
MT-4	200:1	Medium strong	Strong and elastic
MT-9	100:1	Medium strong	Brittle, excessive crosslinking, severe dehydration/23 days
MT-10	50:1	Weak	Extremely brittle, excessive crosslinking, severe dehydration/15 days

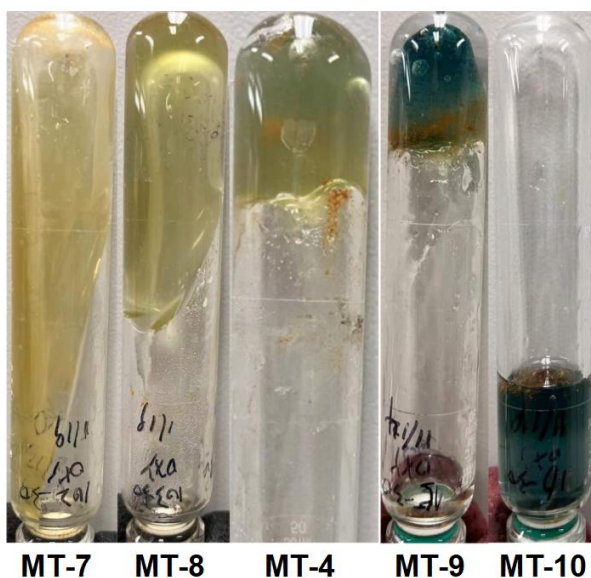


Figure 4.2 Dehydration of MT-RPPG with different concentrations of crosslinker II.

### 4.3. EFFECT OF pH ON MT-RPPG

This section discusses the effect of polymerization pH on the polymerization of the MT-RPPG. Acrylamide might self-crosslinking at low polymerization pH conditions, and the self-crosslinked polymer is inactive to Cr (III). Therefore, low polymerization pH has a negative effect on the re-crosslinking behavior. Furthermore, Cr (III) is unstable at high pH. Severe metal syneresis can be observed when the polymerization pH is higher than 10. In addition, the reactivity of Cr (III) also increases with pH, but the MT-RPPG needs a relatively long re-crosslinking time to avoid too fast re-crosslinking. Therefore, the optimized polymerization pH ranges from 4 to 6.

### 4.4. EFFECT OF CROSSLINKER I ON RPPG PROPERTIES

This section studied the effect of MBA concentration on the swelling kinetics and re-crosslinking behavior of the MT-RPPG.

Table 4.3 The effect of the concentration of MBA on the strength of the primary gel and equilibrium swelling ratio.

#	MBA/ppm	1 <sup>st</sup> gel	Equilibrium swelling ratio/Middle East
MT-4	0	Medium strong	32
MT-11	20	Medium strong	29
MT-12	50	Medium strong	29
MT-13	100	Strong	28
MT-14	200	Brittle	16

Table 4.3 illustrates the effect of MBA on the equilibrium swelling ratio and 1<sup>st</sup> gel strength of the MT-RPPG in Middle East injection water. The 1<sup>st</sup> gel strength

increased with the MBA concentration, but the 1<sup>st</sup> changed from tough gel to brittle gel when the MBA concentration was higher than 100 ppm. Figure 4.3 shows the effect of MBA concentration on the equilibrium swelling ratio of the MT-RPPG. The equilibrium swelling ratio gradually decreases with the increase of MBA concentration, and it drops from 29 to 16 as the MBA concentration increases from 20 to 200 ppm. Figure 4.4 shows the effect of MBA concentration on the re-crosslinking time. The re-crosslinking start and end time increase with the MBA concentration. The re-crosslinking time extended precipitously when the MBA concentration reached 200 ppm. The crosslinking density and rigidity of the polymer gels increase with MBA concentration. Therefore, the polymer gels need more time to become flexible enough to interact with the secondary crosslinker.

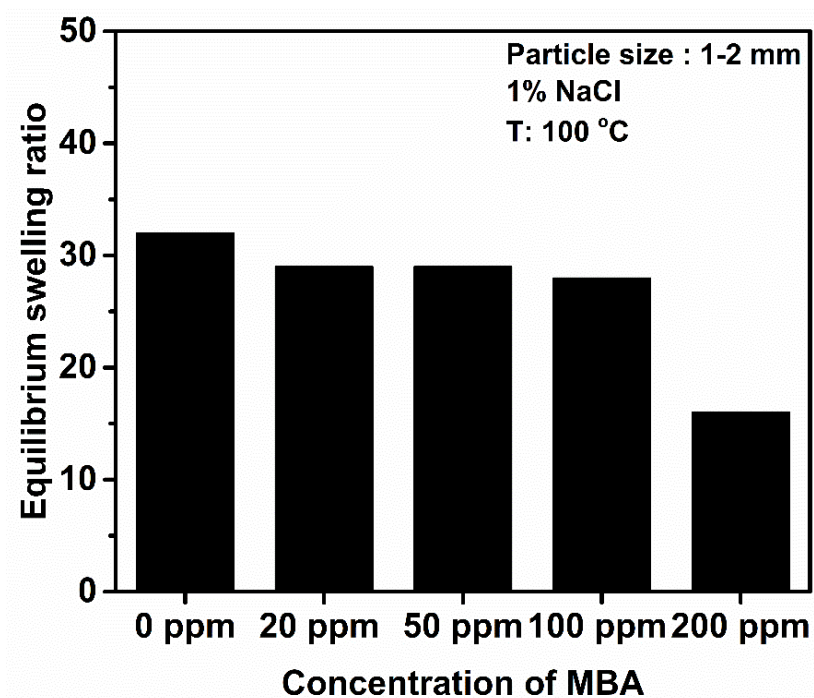


Figure 4.3 The effect of the concentration of MBA effect on the ESR of MT-RPPG.

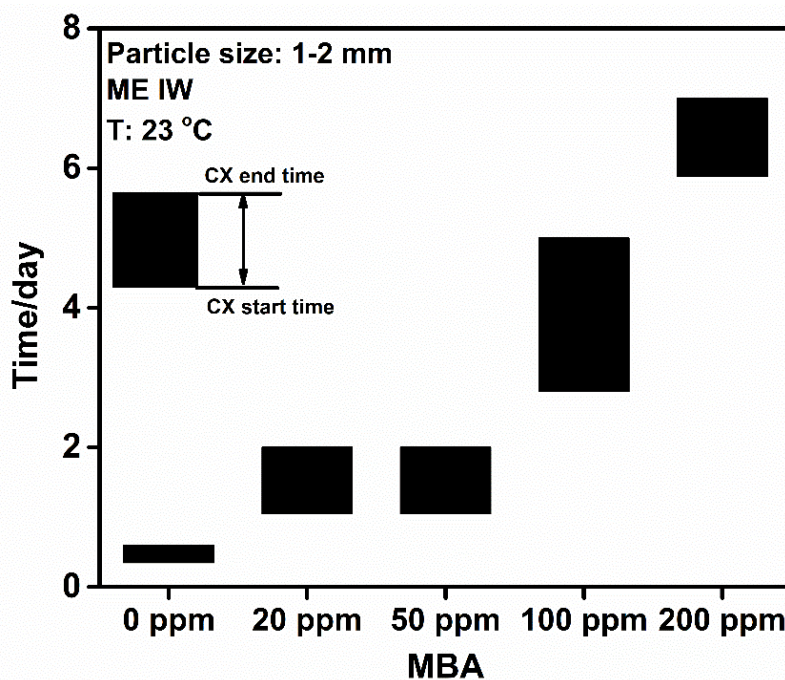


Figure 4.4 The effect of concentrations of MBA on the re-crosslinking time of MT-RPPG.

#### 4.5. SWELLING KINETIC TEST

In this section, we studied the effect of salinity on the swelling kinetics of the MT-RPPG. 1% NaCl, 10% NaCl, 2% KCl, 5% CaCl<sub>2</sub>, and Middle East injection water were used for the swelling kinetic test. Figure 4.5 shows the swelling kinetics results. The equilibrium swelling ratio gradually decreases with the increase of salinity. The MT-RPPG has the fastest swelling rate and highest equilibrium swelling ratio in 1% NaCl. The equilibrium swelling ratios in 1% NaCl, 10% NaCl, 2% KCl, 5% CaCl<sub>2</sub> and Middle East injection water were 29, 29, 27, 18 and 24, respectively. The divalent cations such as Ca<sup>2+</sup> and Mg<sup>2+</sup> significantly affect the equilibrium swelling ratio of the MT-RPPG because of the strong charge shielding effect.

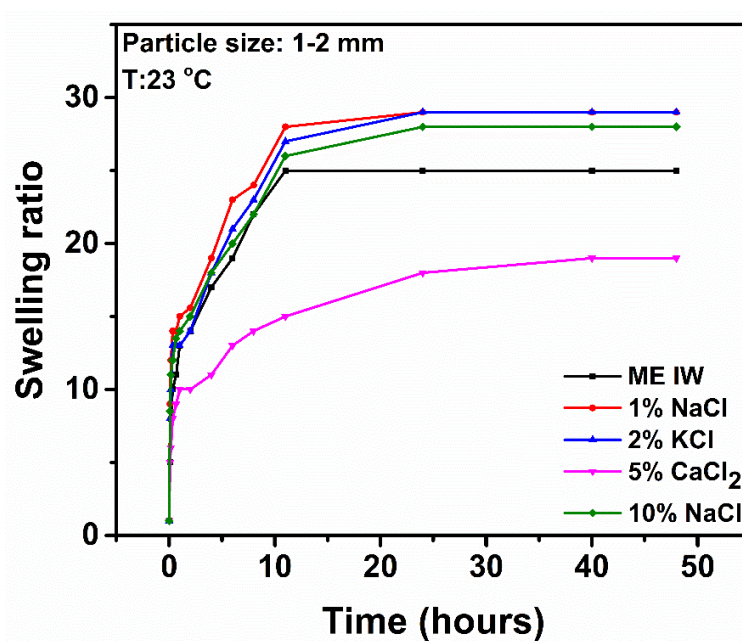


Figure 4.5 Effect of different types of salinities brine on swelling kinetics of the MT-RPPG.

#### 4.6. RHEOLOGY TEST

From the rheology test, we can evaluate the gel strength based on the elastic modulus ( $G'$ ) data. We tested the effect of swelling ratios and salinity on the gel strength. The particle size was 1-2 mm, and the swelling ratios were 10, 20, and 30. 1% NaCl and Middle East injection water were used to prepare the gel slurry. After absorbing all brine water, the gel samples were aged at 100 °C for 2 days before the gel strength test. As depicted in Figure 4.6, the gel strength decreases as the swelling ratio increases. Besides, the gel strength also decreases with the increase of salinity.

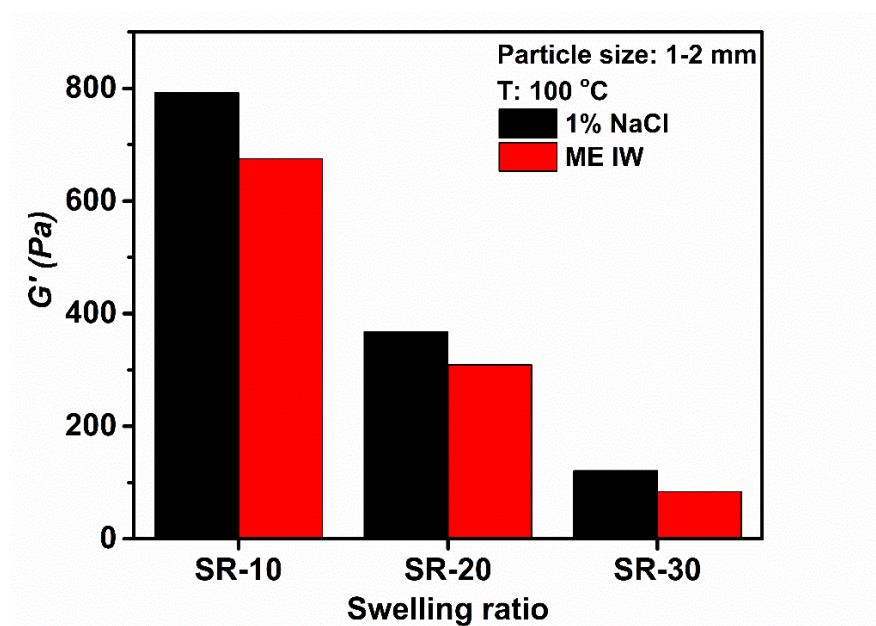


Figure 4.6 Effect of the swelling ratio on the elastic modulus of MT-RPPG.

#### 4.7. THERMOSTABILITY TEST

This section studied the long-term thermal stability of the MT-RPPG. The gel code and gel appearance were recorded periodically. In addition, we also studied the effect of aging time on gel strength.

Figure 4.7 shows the effect of aging time on the gel strength. The gel strength increased precipitously as the extension of aging time. The gel strength increased from 120 Pa to over 1950 Pa after 5 days of aging. However, the gel strength gradually decreases with the extension of aging time. After 100 days of aging, the gel strength decreased to 1154 Pa, and the gel code was I. We think the reason is as follows. The hydrolysis rate of amide groups is significantly accelerated at 100 °C, and more crosslinking points are available for the Cr (III). Therefore, over crosslinking can be observed, and the elastic potential increases with the crosslinking density. The

crosslinked gel must decrease its elastic potential or increase its mixing potential to reach the equilibrium state again. However, we did not observe any water loss or syneresis during the long-term aging test; thus, we think the polymer gel lost its elastic potential by breaking the polymer chains or the crosslinking points. Therefore, the gel strength gradually decreases as crosslinking density decreases or the chain degradations. After reaching the equilibrium state, the gel strength only fluctuates in a small range, and the elastic modulus is maintained around 1100 Pa. Therefore, the MT-RPPG has excellent thermal stability in Middle East injection water at 100 °C.

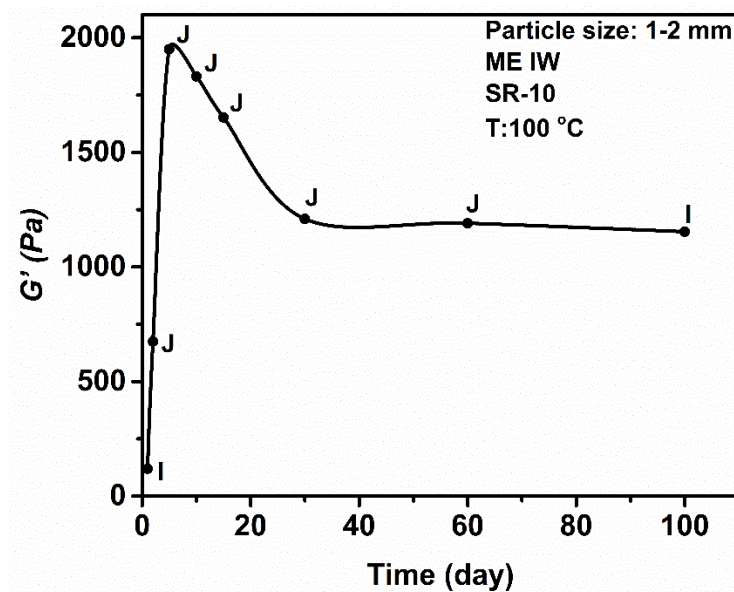


Figure 4.7 Effect of aging time on the strength of MT-RPPG.

Figure 4.8 shows the gel morphology after aging. The MT-RPPG has excellent thermal and phase stability in Middle East injection water. Gels with swelling ratios 20 and 30 maintained their mechanical integrity after 150 days of aging. We did not observe

any syneresis or dehydration during the test. Besides, the MT-RPPG also has excellent phase and thermal stability in concentrated divalent cations solutions. After 60 days of aging, no dehydration was observed in 5 and 10% of  $\text{CaCl}_2$  solutions.

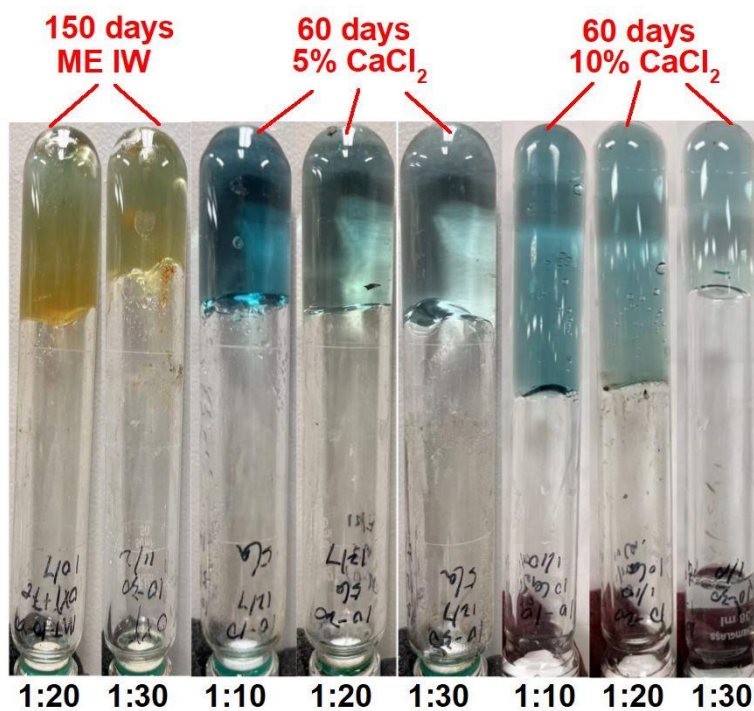


Figure 4.8 The morphology of the MT-RPPG after aging test.

#### 4.8. PLUGGING EFFICIENCY EVALUATION

The core flooding test was performed to test the plugging efficiency of the MT-RPPG. First, the MT-RPPG slurry was injected into the fracture at a constant flow rate of 1.0 mL/min until the pressure became stable. Then, after fully re-crosslinking, the breakthrough test was performed by injecting 1% NaCl at a constant flow rate of 0.5 mL/min. Figure 4.9 shows the water breakthrough pressure result for the MT-RPPG. The



water breakthrough pressure gradient of the MT-RPPG was 118.2 psi/ft, and even after water breakthrough, the MT-RPPG can still provide a relatively high flow resistance to the post-injected fluid. In addition, the average injection pressure gradient was higher than 40 psi/feet, which is higher than the conventional PPG treatment (Pu et al., 2019).

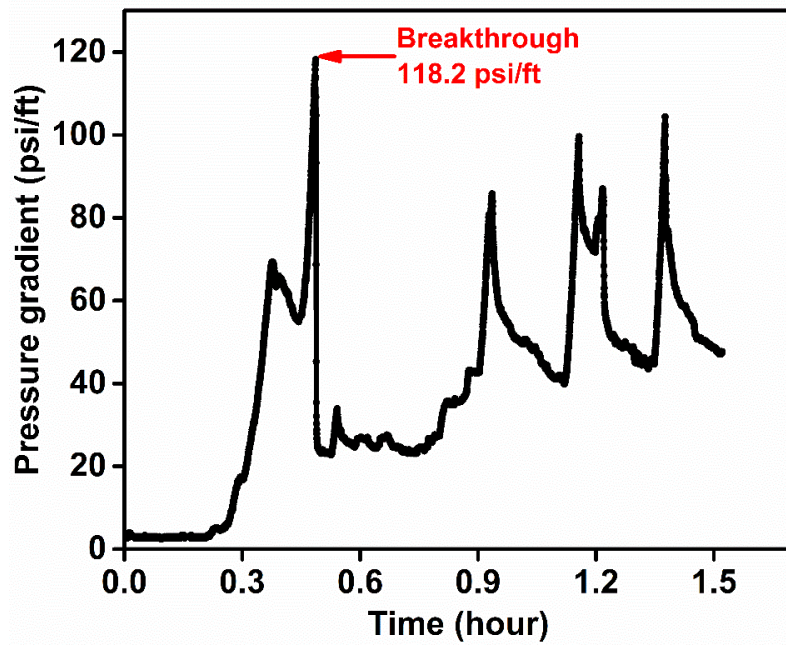


Figure 4.9 Water breakthrough pressure measurement for MT-RPPG during the core flooding test.

After the water breakthrough, the injection rate was adjusted to 0.1, 0.25, 0.5, and 1.0 mL/min, and the stable pressure was recorded to calculate the  $F_{rr}$ . As depicted in Figure 4.10, after the water breakthrough, the  $F_{rr}$  ranges from  $10^8$  to  $10^9$ , and the plugging efficiency is higher than 99.99%.

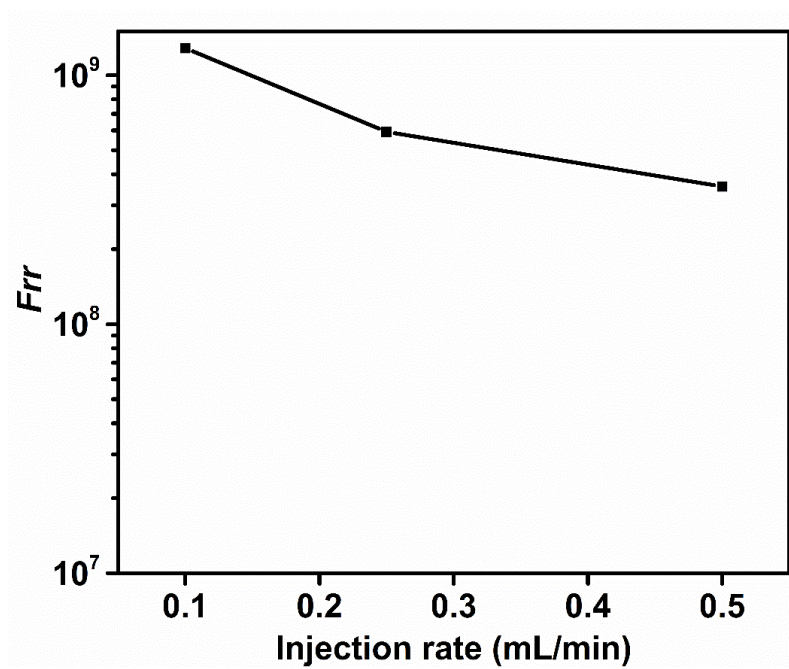


Figure 4.10 Residual resistance factor as a function of injection rate for MT-RPPG.

## **5. SYNTHESIS AND EVALUATION OF ENVIRONMENTALLY FRIENDLY HT-RPPG**

The synthesis process of the Environmentally Friendly HT-RPPG is similar to the MT-RPPG. Compared with the previous HT-RPPGs, this product is cost-effective and easy to scale up. A secondary crosslinker was pre-embed in the gel to endow the PPG with re-crosslinking ability at high temperatures. It was reported that the amine-containing chemical compounds could crosslink the polyacrylamide through the transamidation reaction. PEI and chitosan with a high density of amine groups have been employed to crosslink the polyacrylamide. However, PEI is toxic to aquatic creatures, and chitosan has limited solubility in aqueous solutions, and both crosslinkers are very expensive. Fortunately, we found several cheap amino acids with a high amino density and water solubility that can also crosslink the polyacrylamide. Therefore, we pre-embed the amino acid into polymer gels during the synthesis process and evaluated whether this HT-RPPG can be used in North Sea high-temperature reservoirs conformance control in terms of its swelling kinetics, gel strength, thermal stability and plugging efficiency.

### **5.1. EFFECT OF CROSSLINKER II ON RPPG PROPERTIES**

This section studied the effect of amino acid concentration on the gels' long-term thermal stability. The recipe contains 30 g of AM, 100 g of water, 10 mg of APS and a certain amount of amino acids. As shown in Table 5.1 and Figure 5.1, the 1<sup>st</sup> gel strength gradually decreases with amino acid concentration. The primary gel changed to a flowing gel when the monomer to amino acid weight ratio was lower than 15:1. The amino acid

also acts as a chain transfer agent during the polymerization process, negatively affecting molecular weight. In addition, the chain entanglement decreased with the molecular weight decreased, and the low molecular weight polymer gel cannot form a strong bulk gel after polymerization.

Table 5.1 Effect of the crosslinker II on the strength of the primary gel.

#	M/Crosslinker II	1 <sup>st</sup> gel
HT-1	60:1	Rigid gel
HT-2	30:1	Fixed shape
HT-3	15:1	Flowing
HT-4	10:1	Flowing
HT-5	7.5:1	Highly flowing
HT-6	6:1	Highly flowing

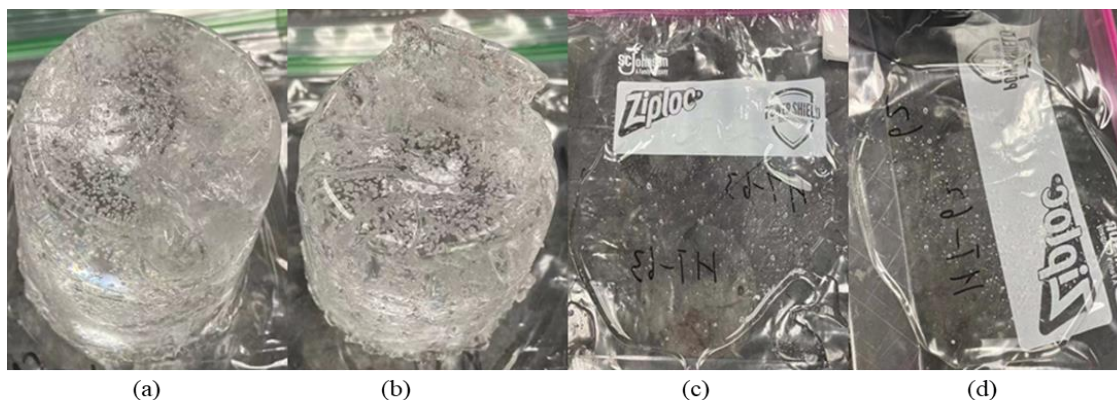


Figure 5.1 The primary bulk gel with different weight ratios of monomers to crosslinker II. (a) 60:1, (b) 30:1, (c) 15:1, (d) 7.5:1.

We also studied the effect of amino acid concentration on the re-crosslinked gel strength. As depicted in Figure 5.2, HT-4 with a swelling ratio of 10 changed to a viscous polymer solution at 130 °C. With the extension of aging time, the viscous polymer

solution gradually changed to a rigid gel after 30 hours of aging. Figure 5.3 shows the effect of amino acid concentration on the gel strength. The elastic modulus of the HT-RPPG with monomer/amino acid weight ratios of 60:1, 30:1, 15:1, 10:1, 7.5:1, and 6:1 were 128, 165, 261, 428, 653, and 1009 Pa. The gel strength gradually increases with the amino acid density. However, the re-crosslinked gel gradually lost its elasticity and became more brittle when the monomer to amino acid weight ratio was lower than 10:1. As a result, the monomer to amino acid weight ratio was fixed at 10:1.



Figure 5.2 Re-crosslinking behavior of the HT-4.

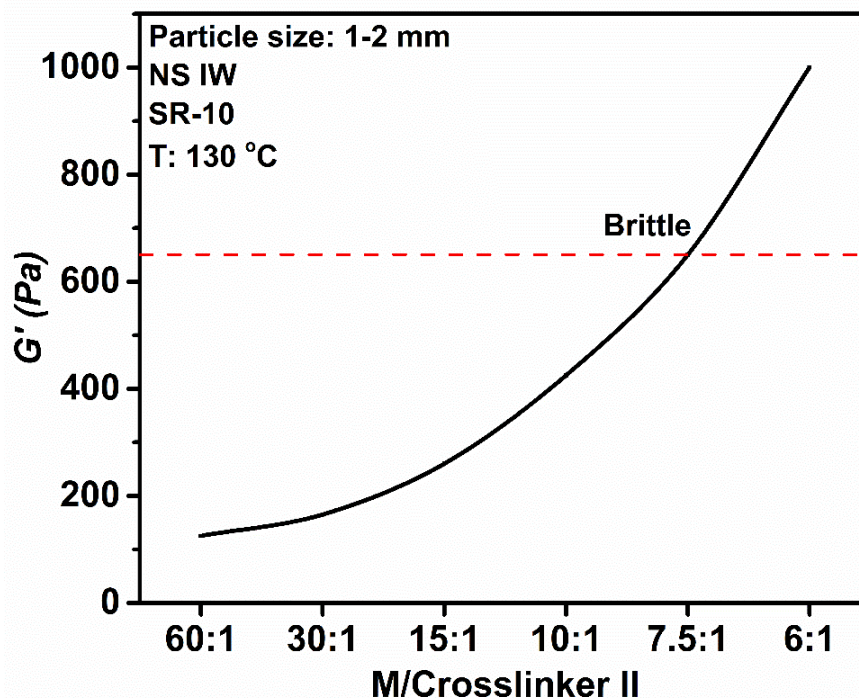


Figure 5.3 Effect of the weight ratios of monomers to crosslinker II on the elastic modulus of HT-RPPG.

## 5.2. EFFECT OF pH ON RPPG PROPERTIES

The solution pH significantly affected the chain transfer efficiency of amino acids, and the chain transfer efficiency decreased with the pH value decreased. Therefore, in this section, we studied the effect of polymerization pH on the gel strength and re-crosslinking ability.

Table 5.2 shows the effect of polymerization pH on the primary gel and re-crosslinked gel strength. The recipe contains 30 g of AM, 100 g of water, 3 g of amino acid, and 10 mg of APS. The primary gels were very robust when the polymerization pH was 4 and 6, and the primary gel strength decreased with the increase of solution pH value. The pristine pH of the monomer and the amino acid solution was 10.3, and the primary gel is highly flowing after polymerization.

However, polymerization pH also has a significant effect on the re-crosslinking behavior. The HT-RPPG failed to re-crosslink when the solution pH was lower than 7, as shown in Figure 5.4. After 2 days of aging, the particle boundaries do not disappear, and the particles can be separated from each other easily. In addition, the swelled gel particles changed to a homogenous gel when the polymerization pH was higher than 7. Therefore, the optimized polymerization pH was 8 to 10.



Figure 5.4 Effect of pH 4, 6, 7, and 8.

Table 5.2 Effect of the pH on the strength of the primary gel and re-crosslinking behavior of the HT-RPPG.

#	pH	1 <sup>st</sup> gel	RX behavior, SR-10, 130 °C North Sea formation water
HT-15	4	Rigid	No
HT-16	6	Rigid	Weak RX, failed to recover it from the tube as a bulky gel
HT-17	7	Fixed shape	RX
HT-18	8	Flowing	RX
HT-19	9	Flowing	RX
HT-7	10.3	Highly Flowing	RX

### 5.3. EFFECT OF CROSSLINKER I ON RPPG PROPERTIES

This section studied the effect of MBA concentration on the HT-RPPG properties. The MBA feeding amount ranges from 0 to 500 ppm. Table 5.3 shows the impact of MBA concentration on the properties of the primary gel. The lowest feeding amount of MBA to achieve a non-flowable primary gel was 100 ppm, and the primary gel strength gradually increased with the MBA feeding amount. The primary gel morphology with different MBA feeding amounts is shown in Figure 5.5.

Table 5.3 Effect of the concentration of MBA on the primary gel strength.

#	MBA/ppm	1 <sup>st</sup> gel
HT-7	0	Flowing
HT-8	10	Flowing
HT-9	20	Flowing
HT-10	50	Flowing
HT-11	100	Fixed shape
HT-12	200	Rigid gel
HT-13	300	Rigid gel
HT-14	500	Rigid gel

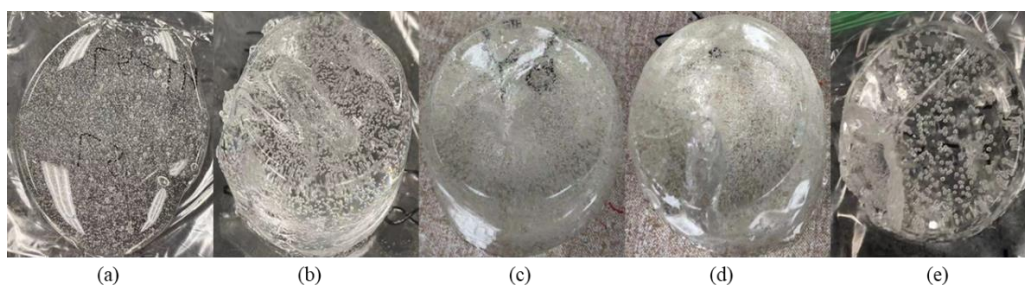


Figure 5.5 The primary gel with different concentrations of MBA.  
 (a) 50 ppm, (b) 100 ppm, (c) 200 ppm, (d) 300 ppm, (e) 500 ppm.



Next, we studied the effect of MBA concentration on the equilibrium swelling ratio of the HT-RPPG in North Sea formation water. As shown in Figure 5.6, the equilibrium swelling ratio decreased with the MBA feeding amount. In addition, for the HT-RPPG with the MBA feeding amount of less than 100 ppm, the equilibrium swelling ratio was higher than 100. The equilibrium swelling ratios of HT-RPPG containing 200, 300, and 500 ppm of MBA were 89, 27, and 20, respectively.

We also studied the effect of the MBA feeding amount on the re-crosslinked behavior of the MT-RPPG. As depicted in Figure 5.7, the re-crosslinked gel strength first increased with MBA, but the further increase in MBA concentration could decrease the gel strength. Therefore, the optimized MBA feeding amount is 300 ppm.

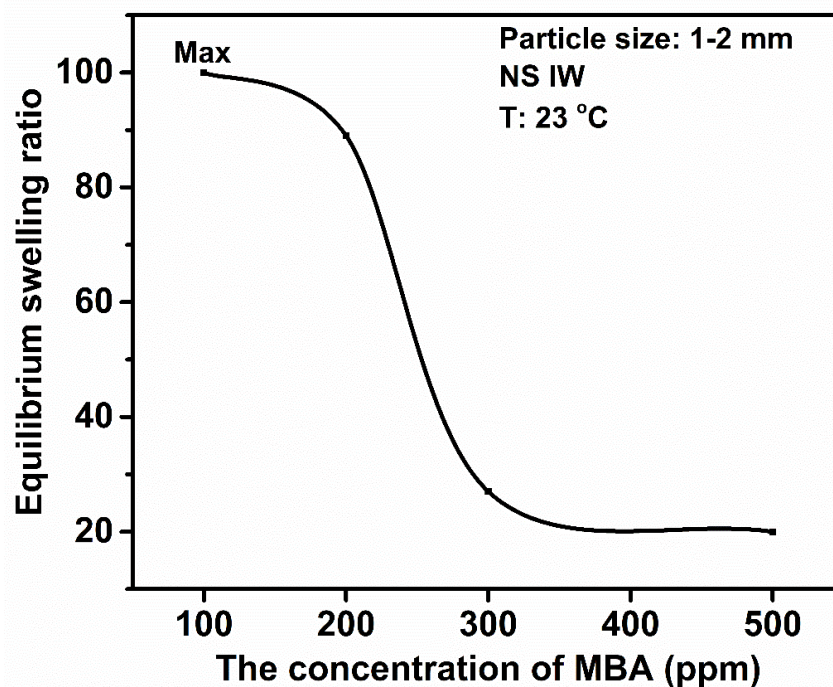


Figure 5.6 Effect of the concentration of MBA on the equilibrium swelling ratio of HT-RPPG.

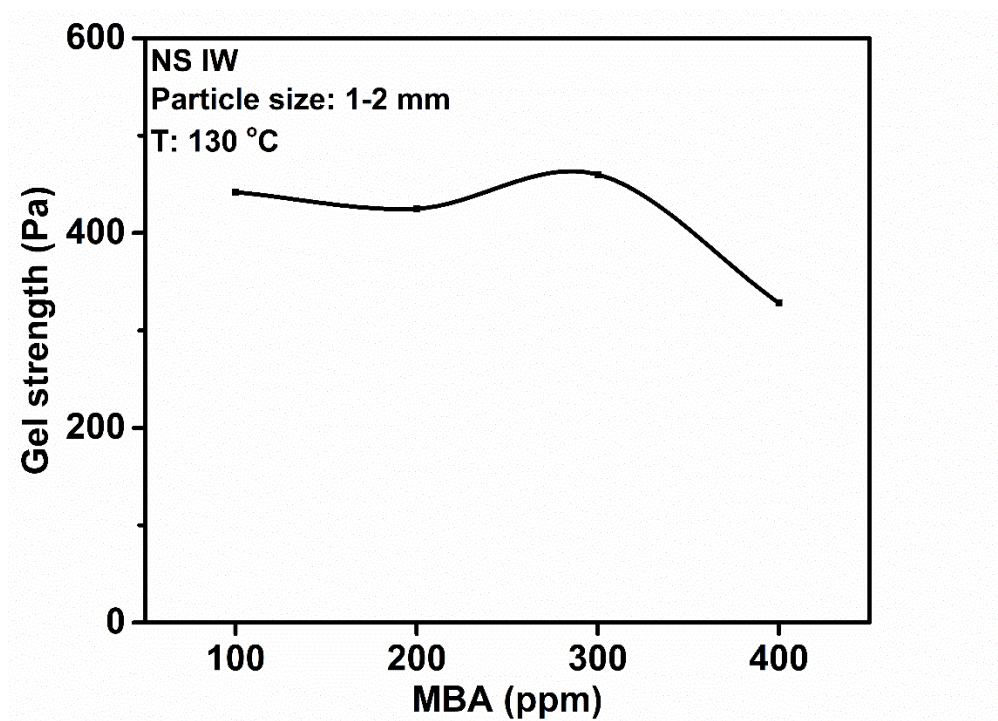


Figure 5.7 Effect of the concentration of MBA on the gel strength of HT-RPPG.

#### 5.4. SWELLING KINETIC TEST

The swelling kinetics of the HT-RPPG at 23 °C are discussed in this section. 1 to 2 mm HT-RPPG particles were swelled in 1% NaCl and North Sea formation water, respectively. Figure 5.8 illustrates the salinity effect on swelling kinetic of HT-RPPG. For the HT-RPPG swelled in 1% NaCl, it reached its half equilibrium swelling ratio after 30 minutes. The HT-RPPG reached its equilibrium swelling ratio after 8 hours, and the equilibrium swelling ratio was 34. For the HT-RPPG swelled in North Sea formation water, it reached its half equilibrium swelling ratio after 40 minutes. The HT-RPPG reached its equilibrium swelling ratio after 8 hours, and the equilibrium swelling ratio was 27.

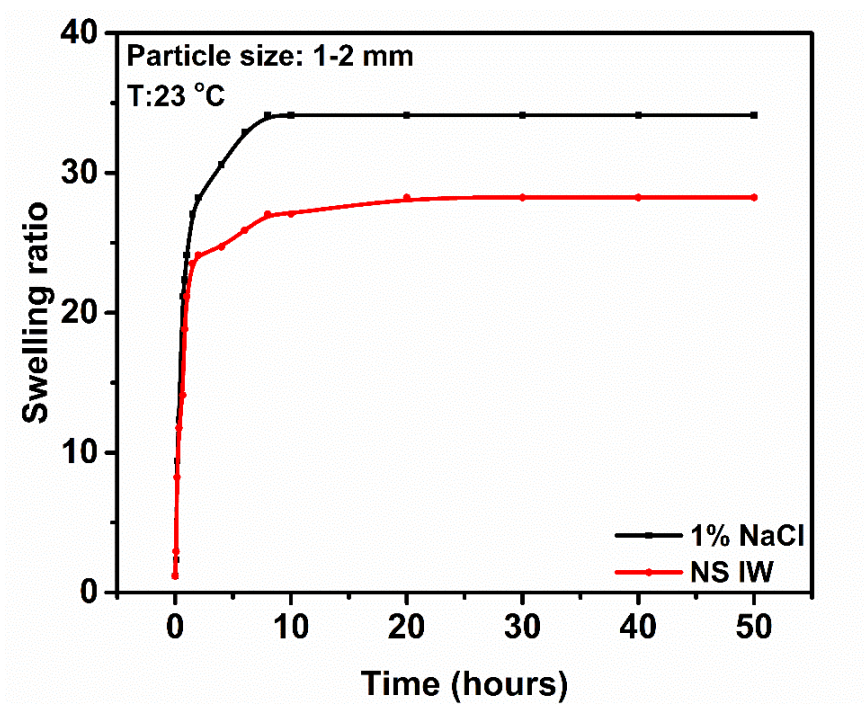


Figure 5.8 Effect of different types of salinities brine on swelling kinetics of the HT-RPPG.

### 5.5. RE-CROSSLINKING TIME TEST

This section studied the effect of swelling ratio and temperature on the re-crosslinking times. The gel particles were swelled in North Sea formation water, and the swelling ratios are 10, half swelling, and equilibrium swelling. The swelled gel was then evaluated for the re-crosslinking time at various temperatures, including 80 °C, 100 °C, and 130 °C. The results of the HT-RPPG re-crosslinking time are shown in Figure 5.9. At 80 °C, the re-crosslinking interval is 4 to 6 days; at 100 °C, it is 28 to 54 hours; and at 130 °C, it is 12 to 18 hours. The results demonstrate that the interval re-crosslinking time decreases as the temperature increases, and the re-crosslinking start time was shortened.

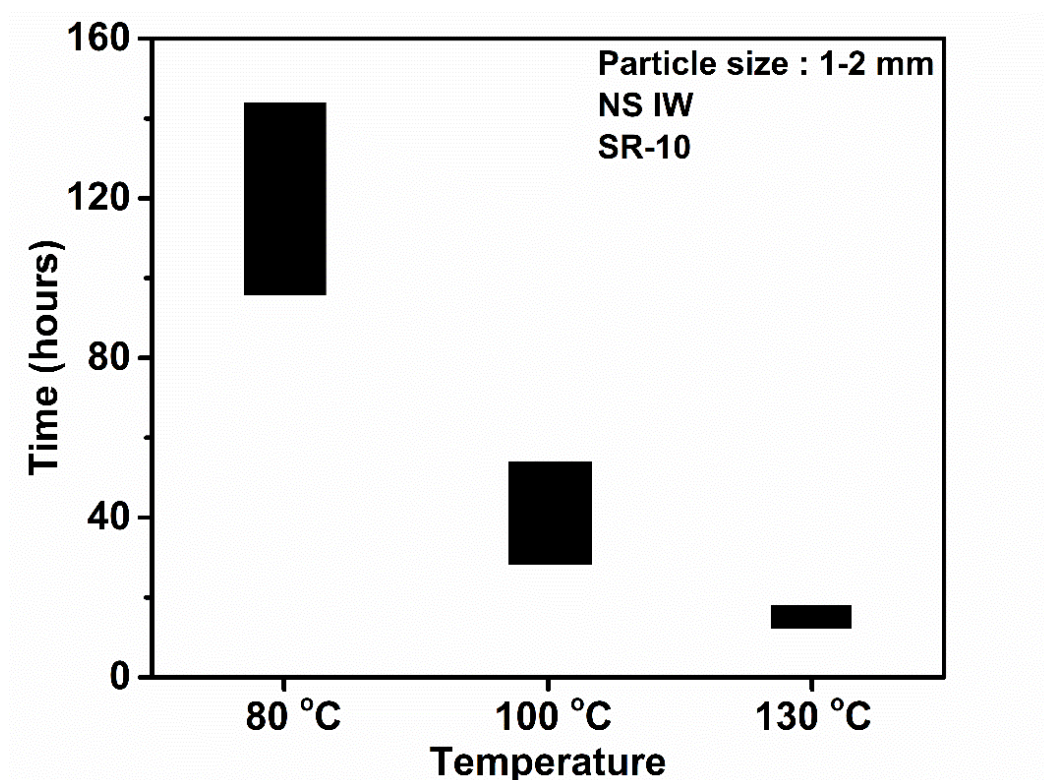


Figure 5.9 Effect of the temperature on the re-crosslinking time of the HT-RPPG with swelling ratio of 10.

## 5.6. RHEOLOGY TEST

This section studied the effect of aging temperatures on gel strength. Figure 5.10 shows the elastic modulus ( $G'$ ) of HT-RPPGs with various swelling ratios at different temperatures. The gel strength increases with aging temperature. For example, the gels with a swelling ratio of 10 has the highest elastic modulus of 460 Pa at 130 °C.

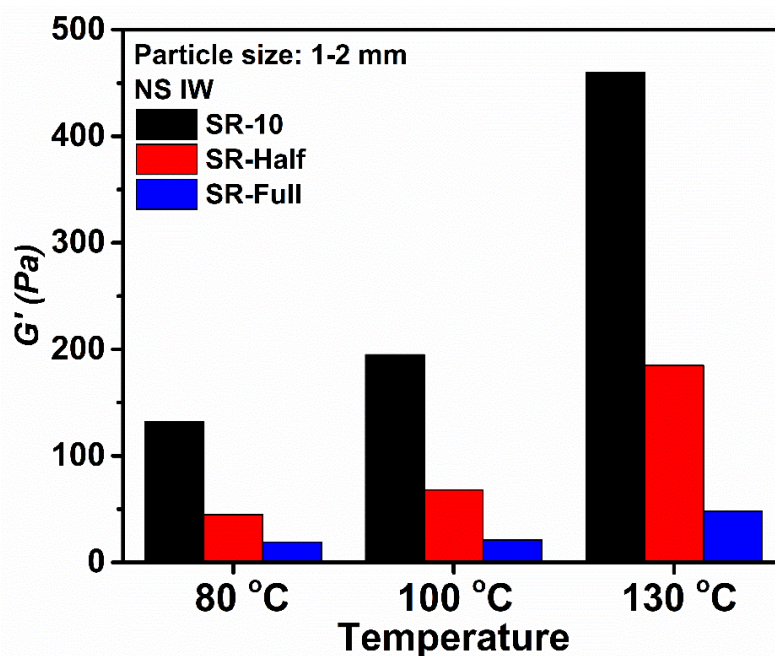


Figure 5.10 Effect of the temperature on the elastic modulus of the HT-RPPG with different swelling ratios.

## 5.7. THERMOSTABILITY TEST

This section evaluates the thermal stability of the HT-RPPG in North Sea formation water at different temperatures. The volume and gel morphology changes were recorded during the aging test. The morphology changes of the HT-RPPG at various temperatures are depicted in Figures 5.11. We did not observe any syneresis or dehydration after 208 days of aging for HT-RPPG with a swelling ratio of 10. Gels still can maintain their mechanical integrity. In addition, the HT-RPPGs with swelling ratio 10/20/30 are stable at 80 °C after 208 days of aging. The retention volume of the HT-RPPGs over time at various temperatures is presented in Figure 5.12. In conclusion, at 80 °C, 100 °C, 120 °C, and 130 °C, the HT-RPPGs with a swelling ratio of 1:10 have excellent long-term phase and thermal stability in North Sea formation water.

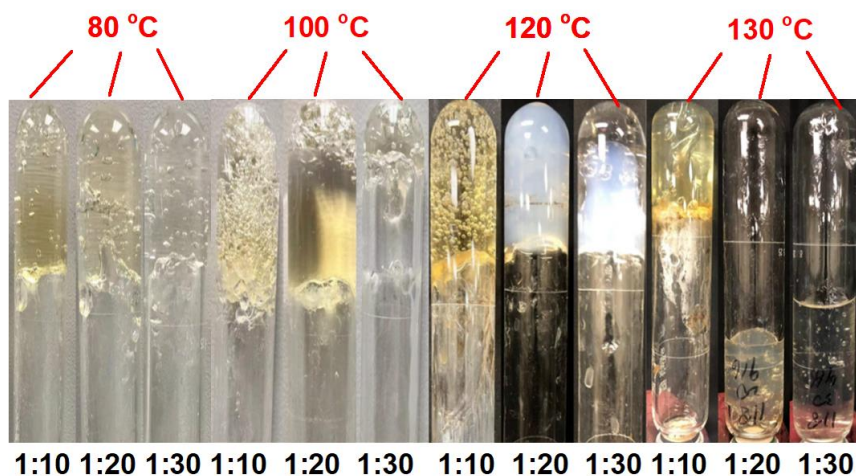


Figure 5.11 The morphology of the HT-RPPG after aging test.

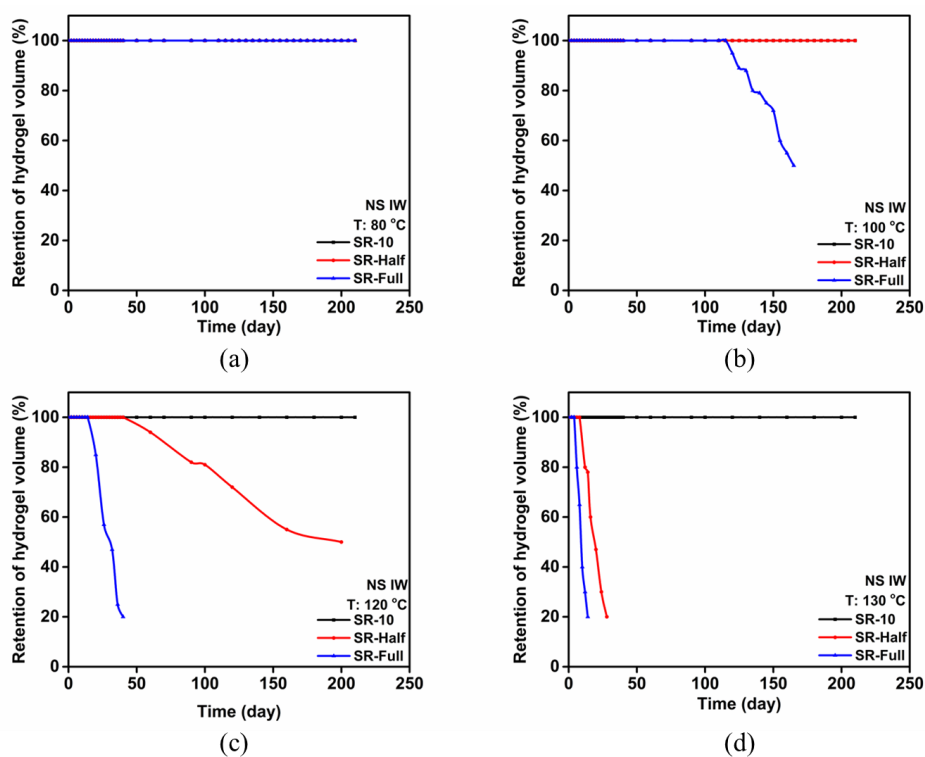


Figure 5.12 Retention volume of the HT-RPPGs with different swelling ratios at 80 °C, 100 °C, 120 °C, and 130 °C. (a) 80 °C, (b) 100 °C, (c) 120 °C, (d) 130 °C.

## 5.8. PLUGGING EFFICIENCY EVALUATION

This section evaluates the plugging efficiency of the HT-RPPG. First, the HT-RPPG slurry was injected into the fracture at a constant flow rate of 1.0 mL/min until the pressure became stable. After that, the core was sealed and aged at 130 °C for 2 days. Then, the breakthrough test was performed by injecting 1% NaCl at a constant flow rate of 0.5 mL/min. The flow rate was changed to 0.1, 0.25, and 0.75 mL/min to calculate the  $F_{rr}$ . As shown in Figure 5.13, the water breakthrough pressure gradient was 68 psi/ft, and after water breakthrough, the injection pressure can be maintained over 30 psi/ft.

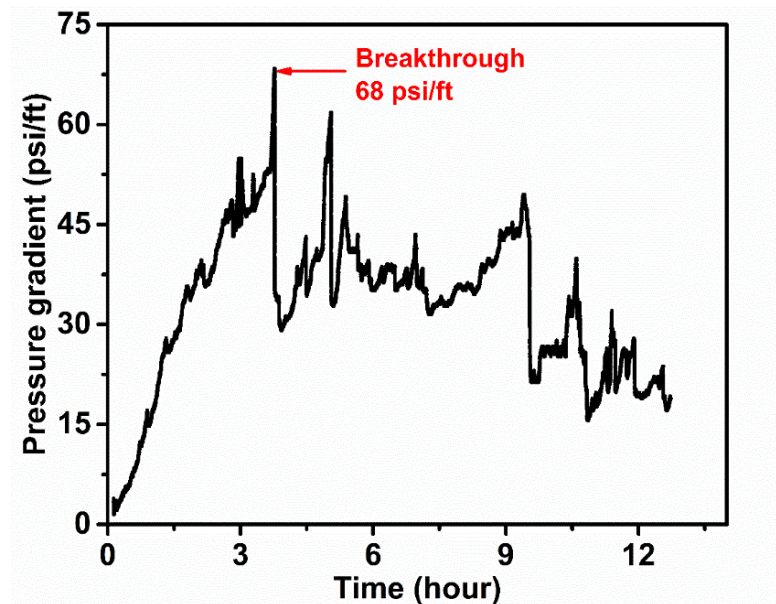


Figure 5.13 Water breakthrough pressure measurement for HT-RPPG during the core flooding test.

The  $F_{rr}$  data are shown in Figure 5.14. The  $F_{rr}$  is more than  $1 \times 10^8$ , and the plugging efficiency is 99.999%.

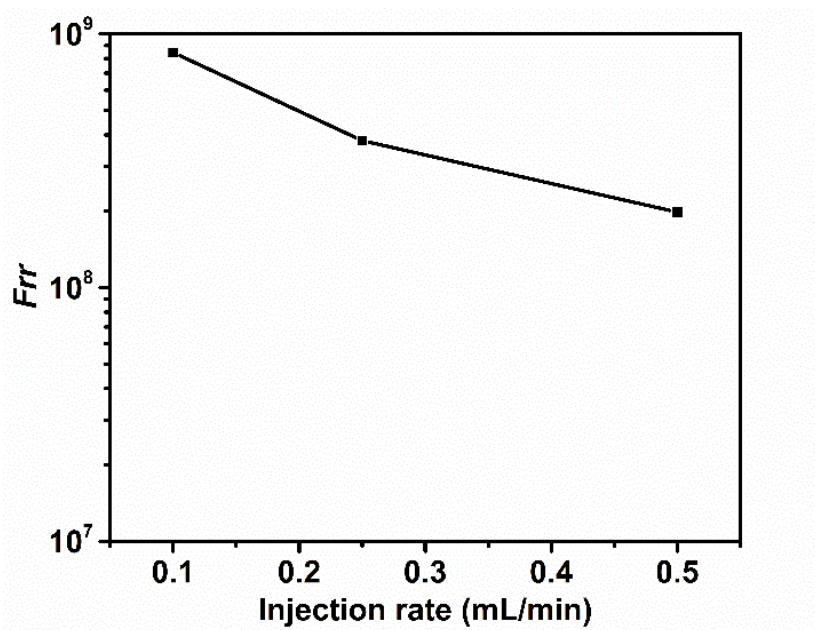


Figure 5.14 Residual resistance factor as a function of injection rate for HT-RPPG.



## 6. CONCLUSIONS

This thesis has developed and systematically evaluated two novel re-crosslinkable preformed particle gels (RPPGs). We successfully developed an MT-RPPG product that can be stable in Middle East injection water for over 150 days at 100 °C. The optimized recipe contains 10 g of AM, 20 g of AMPS, 100 g of water, 10 mg of APS, 0.77 g of  $\text{CrCl}_3 \cdot 6\text{H}_2\text{O}$ , and 20 ppm of MBA. The MT-RPPG has an equilibrium swelling ratio of 24 at ambient temperature in Middle East injection water. The re-crosslinking time ranges from 1 to 2 days. The re-crosslinked gel with the swelling ratio of 1:10 can reach up to 675 Pa. The MT-RPPG also has excellent plugging performance, the breakthrough pressure can reach 118.2 psi/ft, and the plugging efficiency is over 99.99%.

For the HT-RPPG, we successfully embedded the amino acids into the polymer gels, and the swelled gel particle can re-crosslink at temperatures ranging from 80 to 130 °C. The optimized recipe contains 30 g of AM, 100 g of water, 10 mg of APS, 3 g of amino acid, and 300 ppm of MBA. The re-crosslinking time at 130 °C ranges from 12 to 18 hours. The HT-RPPG with a swelling ratio of 10 has been stable in North Sea formation water for 208 days so far at temperatures ranging from 80 to 130 °C. The re-crosslinked gel with a swelling ratio of 10 has an elastic modulus of 460 Pa. The breakthrough pressure was 68 psi/ft.

## 7. RECOMMENDATIONS

A Semi-interpenetrating polymer network (Semi-IPN) is a technique for combining two polymers with differing properties to create a fine morphological composite. One of the components has a linear structure that is crosslinked in the other network structure components. The noncovalent interaction between two polymers can affect the properties of the polymer gels. Therefore, We can further improve the strength of RPPGs by adopting the Semi-IPN structure.

**BIBLIOGRAPHY**

- Al-Muntasheri, G.A., 2012. Conformance control with polymer gels: What it takes to be successful. *Arabian journal for science and engineering*, 37(4): 1131-1141.
- Alvarado, V. and Manrique, E., 2010. Enhanced oil recovery: an update review. *Energies*, 3(9): 1529-1575.
- Bai, B., Huang, F., Liu, Y., Seright, R.S. and Wang, Y., 2008. Case study on preformed particle gel for in-depth fluid diversion, SPE symposium on improved oil recovery. OnePetro.
- Bai, B. et al., 2007a. Conformance control by preformed particle gel: factors affecting its properties and applications. *SPE Reservoir Evaluation and Engineering*, 10(4): 415-421.
- Bai, B., Li, L., Liu, Y., Wang, Z. and Liu, H., 2004. Preformed particle gel for conformance control: factors affecting its properties and applications, SPE/DOE Symposium on Improved Oil Recovery. OnePetro.
- Bai, B., Liu, Y., Coste, J.-P. and Li, L., 2007b. Preformed particle gel for conformance control: transport mechanism through porous media. *SPE Reservoir Evaluation & Engineering*, 10(02): 176-184.
- Bai, B., Wei, M. and Liu, Y., 2013. Field and lab experience with a successful preformed particle gel conformance control technology, SPE production and operations symposium. OnePetro.
- Bai, B., Zhou, J. and Yin, M., 2015. A comprehensive review of polyacrylamide polymer gels for conformance control. *Petroleum exploration and development*, 42(4): 525-532.
- Bailey, B. et al., 2000. Water control. *Oilfield review*, 12(1): 30-51.
- Bera, A. and Mandal, A., 2015. Microemulsions: a novel approach to enhanced oil recovery: a review. *Journal of Petroleum Exploration and Production Technology*, 5(3), pp.255-268.
- Chang, P., Goldman, I. and Stingley, K., 1985. Laboratory studies and field evaluation of a new gelant for high-temperature profile modification, SPE Annual Technical Conference and Exhibition. OnePetro.
- Chauveteau, G. et al., 2001. New size-controlled microgels for oil production, SPE international symposium on oilfield chemistry. OnePetro.

- Chauveteau, G. et al., 2004. Disproportionate permeability reduction by soft preformed microgels, SPE/DOE Symposium on Improved Oil Recovery. OnePetro.
- Chauveteau, G., Tabary, R., Renard, M. and Omari, A., 1999. Controlling in-situ gelation of polyacrylamides by zirconium for water shutoff, SPE International Symposium on Oilfield Chemistry. Society of Petroleum Engineers.
- Cordova, M. et al., 2008. Delayed HPAM gelation via transient sequestration of chromium in polyelectrolyte complex nanoparticles. *Macromolecules*, 41(12): 4398-4404.
- Coste, J.-P. et al., 2000. In-Depth Fluid Diversion by Pre-Gelled Particles. Laboratory Study and Pilot Testing, SPE/DOE improved oil recovery symposium. OnePetro.
- Darcy, H., 1856. *Les fontaines publiques de la ville de Dijon: exposition et application*. Victor Dalmont.
- Darvishi, Z., Kabiri, K., Zohuriaan-Mehr, M. and Morsali, A., 2011. Nanocomposite super-swelling hydrogels with nanorod bentonite. *Journal of Applied polymer science*, 120(6): 3453-3459.
- De, S.K. et al., 2002. Equilibrium swelling and kinetics of pH-responsive hydrogels: Models, experiments, and simulations. *Journal of Microelectromechanical systems*, 11(5): 544-555.
- Dupuis, G., Bouillot, J., Templier, A. and Zaitoun, A., 2015. Successful chemical water shut-off treatment in an omani field heavy-oil well, Abu Dhabi International Petroleum Exhibition and Conference. OnePetro.
- Frampton, H. et al., 2004. Development of a novel waterflood conformance control system, Spe/doe Symposium on Improved Oil Recovery. OnePetro.
- Ghriga, M.A. et al., 2019. Review of recent advances in polyethylenimine crosslinked polymer gels used for conformance control applications. *Polymer Bulletin*: 1-29.
- Green, D.W. & Willhite, G.P. (1998). *Enhanced Oil Recovery*. SPE Textbook Series Vol. 6.
- Hardy, M., Botermans, W., Hamouda, A., Valdal, J. and Warren, J., 1999. The first carbonate field application of a new organically crosslinked water shutoff polymer system, SPE International Symposium on Oilfield Chemistry. Society of Petroleum Engineers.

- Johnson, S. et al., 2010. Effects of divalent cations, seawater, and formation brine on positively charged polyethylenimine/dextran sulfate/chromium (III) polyelectrolyte complexes and partially hydrolyzed polyacrylamide/chromium (III) gelation. *Journal of applied polymer science*, 115(2): 1008-1014.
- Jouenne, S., 2020. Polymer flooding in high temperature, high salinity conditions: Selection of polymer type and polymer chemistry, thermal stability. *Journal of Petroleum Science and Engineering*, 195: 107545.
- Kumar, A., Mahto, V. and Sharma, V.P., 2019. Development of fly ash reinforced nanocomposite preformed particle gel for the control of excessive water production in the mature oil fields. *Oil & Gas Science and Technology–Revue d'IFP Energies nouvelles*, 74: 8.
- Lantz, M. and Muniz, G., 2014. Conformance Improvement Using Polymer Gels: A Case Study Approach, SPE Improved Oil Recovery Symposium. OnePetro.
- Liang, J.-T., Lee, R. and Seright, R., 1993. Gel placement in production wells. *SPE Production & Facilities*, 8(04): 276-284.
- Liu, Y., Bai, B. and Shuler, P.J., 2006. Application and development of chemical-based conformance control treatments in China oilfields, SPE/DOE Symposium on Improved Oil Recovery. OnePetro.
- Liu, Y., Bai, B. and Wang, Y., 2010. Applied technologies and prospects of conformance control treatments in China. *Oil & Gas Science and Technology–Revue d'IFP Energies nouvelles*, 65(6): 859-878.
- Long, Y., Wang, Z., Ding, H., Geng, J. and Bai, B., 2019. Investigation and Characterization of a Robust Nanocomposite Preformed Particle Gel for Enhanced Oil Recovery. *Energy & Fuels*, 33(6): 5055-5066.
- Moradi-Araghi, A., 2000. A review of thermally stable gels for fluid diversion in petroleum production. *Journal of Petroleum Science and Engineering*, 26(1-4): 1-10.
- Moradi-Araghi, A., Cleveland, D. and Westerman, I., 1987. Development and evaluation of eor polymers suitable for hostile environments: II-Copolymers of acrylamide and sodium AMPS, SPE International Symposium on Oilfield Chemistry. OnePetro.
- Morgan, J., Smith, P. and Stevens, D., 1997. Chemical adaptation and development strategies for water and gas shutoff gels, RSC chemistry in the oil industry, 6th international symposium, Charlotte Mason College Ambleside, UK.

- Nanda, S., Kumar, R., Sindhwani, K. and Goyal, K., 1987. Characterization of Polyacrylamine-Cr+6 Gels Used for Reducing Water/Oil Ratio, SPE International Symposium on Oilfield Chemistry. OnePetro.
- Ohms, D. et al., 2010. Incremental-oil success from waterflood sweep improvement in Alaska. SPE Production & Operations, 25(03): 247-254.
- Peng, B. et al., 2018. Applications of nanotechnology in oil and gas industry: Progress and perspective. The Canadian journal of chemical engineering, 96(1): 91-100.
- Pritchett, J. et al., 2003. Field application of a new in-depth waterflood conformance improvement tool, SPE international improved oil recovery conference in Asia Pacific. OnePetro.
- Pu, J. et al., 2019. A recrosslinkable preformed particle gel for conformance control in heterogeneous reservoirs containing linear-flow features. SPE Journal, 24(04): 1714-1725.
- Qiu, Y., Wei, M. and Bai, B., 2017. Descriptive statistical analysis for the PPG field applications in China: Screening guidelines, design considerations, and performances. Journal of Petroleum Science and Engineering, 153: 1-11.
- Qiu, Y., Wu, F., Wei, M., Kang, W. and Li, B., 2014. Lessons learned from applying particle gels in mature oilfields, SPE Improved Oil Recovery Symposium. OnePetro.
- Rousseau, D. et al., 2005. Rheology and transport in porous media of new water shutoff/conformance control microgels, SPE international symposium on oilfield chemistry. OnePetro.
- Saghafi, H.R., Naderifar, A., Gerami, S. and Emadi, M.A., 2016. Improvement in thermo-chemical stability of nanocomposite preformed particle gels for conformance control in harsh oil reservoir conditions. The Canadian Journal of Chemical Engineering, 94(10): 1880-1890.
- Salimi, F., Sefti, M.V., Jarrahian, K., Rafipoor, M. and Ghorashi, S.S., 2014. Preparation and investigation of the physical and chemical properties of clay-based polyacrylamide/Cr (III) hydrogels as a water shut-off agent in oil reservoirs. Korean Journal of Chemical Engineering, 31(6): 986-993.
- Scoggins, M. and Miller, J., 1979. Determination of water-soluble polymers containing primary amide groups using the starch-triiodide method. Society of Petroleum Engineers Journal, 19(03): 151-154.

- Seright, F.S. and Martin, F.D., 1991. Fluid diversion and sweep improvement with chemical gels in oil recovery processes, New Mexico Inst. of Mining and Technology, Socorro, NM (USA). New Mexico ....
- Sheng, J. J. (2011). Modern chemical enhanced oil recovery: Theory and practice. Burlington, Mass.: Gulf Professional Publ
- Singh, R., Mahto, V. and Vuthaluru, H., 2018. Development of a novel fly ash-polyacrylamide nanocomposite gel system for improved recovery of oil from heterogeneous reservoir. *Journal of Petroleum Science and Engineering*, 165: 325-331.
- SONG, X.-w., CAO, X.-l., CHI, Q.-s., LI, D.-x. and HOU, J.-r., 2010. Research on profile control and water shut-off performance of pre-crosslinked gel particles and matching relationship between particle and pore size. *Advances in Natural Science*, 2(2): 36-46.
- Stahl, G.A. and Schulz, D., 1988. Water-soluble polymers for petroleum recovery. Springer Science & Business Media.
- Sydansk, R.D., 1988. A new conformance-improvement-treatment chromium (III) gel technology, SPE enhanced oil recovery symposium. OnePetro.
- Sydansk, R.D., 1990. A newly developed chromium (III) gel technology. *SPE Reservoir Engineering*, 5(03): 346-352.
- Sydansk, R.D. and Romero-Zerón, L., 2011. Reservoir conformance improvement. Society of Petroleum Engineers Richardson, TX.
- Targac, G. et al., 2020. Case History of Conformance Solutions for West Sak Wormhole/Void Space Conduit with a New Reassembling Pre-formed Particle Gel RPPG, SPE Annual Technical Conference and Exhibition. OnePetro.
- Tongwa, P. and Bai, B., 2014. Degradable nanocomposite preformed particle gel for chemical enhanced oil recovery applications. *Journal of Petroleum Science and Engineering*, 124: 35-45.
- Tongwa, P., Nygaard, R. and Bai, B., 2013. Evaluation of a nanocomposite hydrogel for water shut-off in enhanced oil recovery applications: Design, synthesis, and characterization. *Journal of Applied Polymer Science*, 128(1): 787-794.
- Van Hung, N., Quy, N.M. and Long, H., 2020. Enhanced oil recovery: a selection technique for the energy and recovery of Bach Ho field in Vietnam, CIGOS 2019, Innovation for Sustainable Infrastructure. Springer, pp. 733-738.

- Veil, J., 2015. US produced water volumes and management practices in 2012. Groundwater Protection Council.
- Wang, Z. and Bai, B., 2018. Preformed-particle-gel placement and plugging performance in fractures with tips. *SPE Journal*, 23(06): 2316-2326.
- Young, T., Willhite, G. and Green, D., 1988. Study of intra-molecular crosslinking of polyacrylamide in Cr (III)-Polyacrylamide gelation by size-exclusion chromatography, low-angle laser light scattering, and viscometry, *Water-Soluble Polymers for Petroleum Recovery*. Springer, pp. 329-342.
- Yu, B., Zhao, S., Long, Y., Bai, B. and Schuman, T., 2022. Comprehensive evaluation of a high-temperature resistant re-crosslinkable preformed particle gel for water management. *Fuel*, 309: 122086.
- Zaitoun, A. and Dupuis, G., 2017. Conformance control using SMG microgels: laboratory evaluation and first field results, SPE Europec featured at 79th EAGE Conference and Exhibition. OnePetro.
- Zaitoun, A. et al., 2007. Using microgels to shut off water in a gas storage well, International Symposium on Oilfield Chemistry. OnePetro.
- Zhao, H., Zhao, P., Bai, B., Xiao, L. and Liu, L., 2006. Using associated polymer gels to control conformance for high temperature and high salinity reservoirs. *Journal of Canadian Petroleum Technology*, 45(05).
- Zhu, D., Bai, B. and Hou, J., 2017. Polymer gel systems for water management in high-temperature petroleum reservoirs: a chemical review. *Energy & fuels*, 31(12): 13063-13087.



## VITA

Zhanmiao Zhai received his Bachelor of Science in Petroleum Engineering from Northeast Petroleum University and Missouri University of Science and Technology in May 2020. In 2020, he joined the research group of Dr. Baojun Bai and started to pursue his master's degree. In May of 2022, Zhanmiao received his Master of Science in Petroleum Engineering from Missouri University of Science and Technology.